Energy Conversion and Management 284 (2023) 116968

Contents lists available at ScienceDirect

Energy Conversion and Management

journal homepage: www.elsevier.com/locate/enconman

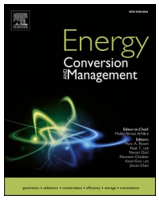

Techno-economic analysis of a combined heat and power system integrating hybrid photovoltaic-thermal collectors, a Stirling engine and energy storage

Shunmin Zhu [a,b], Kai Wang [c], Iker González-Pino [d], Jian Song [a], Guoyao Yu [b], Ercang Luo [b,*], Christos N. Markides [a,*]

[a] Clean Energy Processes (CEP) Laboratory, Department of Chemical Engineering, Imperial College London, South Kensington Campus, London SW7 2AZ, UK
[b] Key Laboratory of Cryogenics, Technical Institute of Physics and Chemistry, Chinese Academy of Sciences, Beijing 100190, China
[c] Institute of Refrigeration and Cryogenics, Zhejiang University, Hangzhou 310027, China
[d] ENEDI Research Group, Department of Energy Engineering, Faculty of Engineering of Bilbao, University of the Basque Country UPV/EHU, Plaza Torres Quevedo 1, Bilbao 48013, Spain

ARTICLE INFO

Keywords:
Energy conversion
Energy storage
Combined heat and power
Photovoltaic-thermal collector
Stirling engine

ABSTRACT

This paper presents a comprehensive analysis of the energetic, economic and environmental performance of a micro-combined heat and power (CHP) system that comprises 29.5 m^2 of hybrid photovoltaic-thermal (PVT) collectors, a 1-kW_e Stirling engine (SE) and energy storage. First, a model for the solar micro-CHP system, which includes a validated transient model for the SE micro-CHP unit, is developed. Parametric analyses are performed throughout a year to evaluate the effects of key component sizes and operating parameters, including collector flow rate, storage tank size, SE micro-CHP flow rate, and battery capacity, on the energetic, economic and environmental performance of the proposed system using real hourly weather data, and thermal and electrical energy demand profiles of a detached house located in London (UK). The optimum component sizes and operating parameters are determined accordingly. The daily and monthly operating characteristics of the system are evaluated, and its annual performance is compared to those of a reference system (gas boiler plus grid electricity), as well as of other alternative solar-CHP systems including a PVT-assisted heat pump system and a standalone PVT system. The results indicate that the installation of such a system can achieve an annual electricity self-sufficiency of 87% and an annual thermal energy demand coverage of 99%, along with annual primary energy savings and carbon emission reduction rate of 35% and 37% relative to the reference system. Over 30 years of operation, the net present value (NPV) of the proposed system is £1990 and the discounted payback period is 28 years. The economics of the proposed system is very sensitive to utility prices, especially the electricity purchase price. Relative to the alternative solar systems, the proposed system offers greater environmental benefits but has a longer payback period. This implies that although the energy saving and emission reduction potential of the proposed system is significant, the initial/capital investment, especially of the SE CHP unit and the PVT collector array, are currently high, so efforts should focus on the cost reduction of these technologies.

1. Introduction

Energy consumption in the building sector is high relative to others. Taking the UK as an example, heating and hot water for buildings account for 40% of energy use and 20% of greenhouse gas emissions [1]. Therefore, the building sector has a great potential to contribute to the UK's greenhouse gas emission reduction targets. Increasing the penetration of renewable energy sources and enhancing primary energy efficiency are becoming more significant in this sector.

Among different renewable energies, though depending on meteorological conditions, solar energy is a prominent source as it is infinite, easily available, and non-polluting. Hence the utilisation of solar energy is a key enabler for the transition to a clean and sustainable energy future. In the past decades, both solar thermal collectors (STCs) and photovoltaic (PV) panel installations have significantly increased their

* Corresponding authors.
E-mail addresses: ecluo@mail.ipc.ac.cn (E. Luo), c.markides@imperial.ac.uk (C.N. Markides).

https://doi.org/10.1016/j.enconman.2023.116968
Received 16 January 2023; Received in revised form 3 March 2023; Accepted 24 March 2023
Available online 30 March 2023

Nomenclature

Abbreviations

AB	auxiliary boiler
CHP	combined heat and power
DHW	domestic hot water
ESS	electricity self-sufficiency
FiT	feed-in tariffs
ICE	internal combustion engine
NPV	net present value
PV	photovoltaic
PVT	photovoltaic-thermal
RFC	reference flow conditions
SE	Stirling engine
SEG	Smart Export Guarantee
SoC	state-of-charge
SP	space heating
STC	solar thermal collector
TSS	thermal energy self-sufficiency

Symbols

A_{cT}	total PVT collector area, m^2
c_e	unit electricity price, £/kWh
c_{ng}	unit natural gas price, £/kWh
CF_n	annual net saving in the nth year, £
CI_{ge}	carbon emission factors for grid electricity, $kgCO_{2\text{-eq}}$/kWh
CI_{ng}	carbon emission factors for natural gas, $kgCO_{2\text{-eq}}$/kWh
d	discount rate, %
E	electricity, kWh
EC	emitted carbon, $kgCO_{2\text{-eq}}$
G	annual gas consumption, kWh
G_{ref}	incident irradiance at reference conditions, W/m^2
G_T	global solar irradiance, W/m^2
i	inflation rate, %
INV	additional initial investment, £
M	annual maintenance cost, £
q_u	useful heat flow, W/m^2
Q	thermal energy, kWh
R	replacement cost, £
$RefE_\eta$	efficiency for separate power production, %
$RefQ_\eta$	efficiency for separate heat production, %
SEG_{tariff}	Smart Export Guarantee tariff, £/kWh
T	temperature, ℃
T_a	ambient temperature, ℃
T_{fm}	mean fluid temperature, ℃
T_r	reduced temperature, ℃
T_{ref}	cell temperature at reference conditions, ℃
T_{PV}	photovoltaic cell temperature, ℃
V_t	storage tank volume, L
β_r	temperature coefficient of solar cell efficiency
β_G	incident radiation coefficient of solar cell efficiency
η_{ref}	electrical efficiency at reference conditions, %
η_{PV}	photovoltaic efficiency, %
ΔCO_2	equivalent CO_2 avoided emission, %

Subscripts

ref	reference system
export	exported
import	imported
n	node, nth year
out	outlet
pro	proposed system
supply	supplied
SECHP	Stirling engine micro-CHP unit

presence in the domestic applications. Compared to PV panel installations and STCs, photovoltaic-thermal (PVT) collectors are an emerging solar energy utilisation technology with a small market share [2]. A typical PVT collector comprises a PV module laminated on top of a thermal absorber for heat removal, which makes it capable of providing both heat and electricity from the same collector area. PVT collectors solve the issue related to conversion efficiency deterioration experienced at elevated operation temperatures for conventional PV panels effectively, by cooling PV panels with a flow of heat transfer fluid (water, glycol, mineral oil or air) that is then used for space heating (SP) or provision of domestic hot water (DHW). Therefore, increasing interest has been drawn into this field in recent years, mainly concentrating on PVT collector modelling [3], test [4,5], performance improvement [6–8], techno-economic assessments for different building applications [9–11], and so on [12]. PV panels, STCs, and PVT collectors are all based on the solar radiation incident on the panels or collectors during daylight, and they rely on energy storage (thermal energy storage and/or electrical energy storage) to fulfil load demands during the night hours and low-irradiance periods. In addition, with the massive deployment of PVT collectors and PV panels (above a threshold installed capacity), the produced electricity feeding into the grid will induce difficulties in the operation and balancing of the national electricity transmission system [13], and it is suggested that the introduction of additional electricity storage would mitigate these issues [13,14].

On the other hand, combined heat and power (CHP) systems improve the overall plant efficiency as it allows heat recovery in electricity production [15]. Hence the global drive for increased primary energy efficiency has led to a continually growing development of such systems in recent years. Unlike the centralised nature of large-scale CHP systems (generally with an electrical capacity above 1 MW [15]), micro-CHP systems (with an electrical capacity below 15 kW [16]) are decentralised energy systems producing heat and electricity simultaneously at the point of use, and thereby reducing the demands on costly energy distribution infrastructure and avoiding energy long-distance transmission losses. This makes micro-CHP systems particularly promising for distributed deployment in domestic applications. The currently available micro-CHP technologies can be classified into two main categories, namely: (i) technologies based on thermodynamic cycles; and (ii) technologies not based on thermodynamic cycles [15]. The former includes micro-gas turbines, internal combustion engines (ICEs), Stirling engines (SEs), and Rankine cycle-based systems, while the latter mainly includes fuel cell-based systems. It should be noted that the aforementioned PVT collectors can also be regarded as a micro-CHP technology that is not based on thermodynamic cycles. Among these micro-CHP technologies, SE micro-CHP technologies have the advantages of low emissions, low maintenance costs, low noise, and low vibration, high thermal-to-electrical efficiency, and flexibility of fuel sources [17–19], which makes them well suited for residential applications and utilisation of renewable energy sources (such as solar energy and biomass) at a small- or micro-scale [20].

In recent years, higher household energy bills and a desire to transition to a low-carbon fuel supply for the provision of heating and power have catalysed an interest in the integration of solar energy with engine-based cogeneration systems [21–25]. The benefits of such technologies, include: (i) the introduction of solar energy reduces the consumption of fossil fuels, which will reduce household energy bills directly; and (ii) the addition of engine-based cogeneration units to a solar system reduces the required capacity of energy storage for a standalone solar system to some extent [21]. Brandoni et al. [22] investigated an integrated system consisting of PV (or high concentration PV) and micro-

CHP devices for dwelling sector applications, with results addressing the importance of optimal sizing of such a system for maximising the economic and energy savings with respect to conventional approaches. In a Spanish case study, Rodríguez et al. [23] studied the use of a system that comprised STCs, PV panels and natural gas-fuelled ICEs for a six-storey residential block. The results showed that though the life cycle cost of the proposed system is the highest among all considered systems, both the primary energy consumption reduction and emission reduction potential of the proposed system is the highest. Shah et al. [24] studied the performance of PV-battery-ICE systems located in three representative regions of the US, and the results indicated that with reasonably sized components, such integrated systems are technically viable in any continental American climate. Later, Mundada et al. [25] from the same group further estimated the levelised cost of electricity (LCOE) of these systems, in an attempt to quantify their economic viability, and a case study in Houghton of Michigan demonstrated that such systems could already generate a profit for some off-grid consumers.

Due to the better adaptability in domestic environment and better compatibility with renewable energy sources of SE than that of ICE, research which couple SE cogeneration units with PV panels or STCs have also been performed. Karmacharya et al. [26] analysed the performance of a system which included a SE micro-CHP (from Whispergen), micro wind turbine and PV array modules by using an integrated simulation model developed in Matlab/Simulink. Based on the consideration of the UK as a case study, the results showed that the electrical contribution by the SE micro-CHP module was heavily dependent on the thermal demand of the building. Jimenez et al. [27] compared a PV-SE-battery system with a PV-diesel generator/battery system in a rural community of Bolivia, and the results showed that the former outperformed the latter in terms of CO_2 emission reduction, annualised total cost saving and energy saving. Kotowicz et al. [28] studied an integrated energy system combining a SE-based micro-CHP unit (electrical capacity: 1 kW_e, and thermal capacity: 26 kW_{th}) with PV panels and battery, and found that the proposed system could achieve a high level of energy self-sufficiency for the consumer (electrical and thermal energy self-sufficiency may reach up to 99% and 100%, respectively). Balcombe et al. [21] simulated an integrated system comprising SE CHP (electrical capacity: 1 kW_e, and thermal capacity: 24 kW_{th}), solar PV and battery storage in a UK context, which could obtain an increase in electricity self-sufficiency, and indicating that such an integrated system was financially viable for households with electricity demands higher than 4300 kWh/year. In addition, an environmental analysis indicated that such an integrated system could lead to lower environmental impacts compared to a conventional electricity and heat provision approach, and the larger the household energy demand, the greater the environmental benefits [29].

In addition to simulations, some experimental work relating to SE-based CHP systems have also been performed. Auñón-Hidalgo et al. [30] studied an installation combining renewable sources (3.2 kW_e PV modules and two STCs) and a SE micro-CHP unit (electrical capacity: 1 kW_e, and thermal capacity:7 kW_{th}) experimentally; the results showed that with energy storage, the installation could satisfy 75.6% of the total energetic demand for a typical household while achieving a reduction of 36.2% in CO_2 emission when compared with a reference system (grid electricity plus diesel oil boiler). İncili et al. [31] developed and tested a cogeneration system which consisted of PV modules, a SE, and a coal-fired boiler, aiming at satisfying the energy demand of a multi-family house in Turkey. Economic analysis indicated that although the additional cost of the proposed cogeneration system was the highest, both the payback period and the LCOE value of the proposed system were the least among three systems considered in this study.

It can be concluded that the aforementioned studies have focussed on the integration of solar technologies with SE cogeneration units to form CHP systems, specifically employing solar PV modules or a combination of STCs and PV modules. Considering the advantages of hybrid PVT collectors compared to PV modules, or the combination using of STCs and PV modules [10], coupling PVT collectors with a SE cogeneration unit is an interesting option for integrated CHP systems [32]. However, few studies have consdered such systems. This work aims to fill this gap, by investigating the coupling of PVT collectors with a natural gas-powered SE cogeneration unit, and energy storage, for the combined provision of heating and electricity to residential buildings. The purpose of this work is to provide a comprehensive assessment on the proposed system in terms of energetic, economic and environmental potentials. To do so, a transient model which can be used to predict the operation and performance of the proposed system is developed. A transient sub-model for the SE micro-CHP unit, considering the start-up and shut-down dynamics of the unit is integrated with the transient model, which is usually neglected in previous research [32] while is important to capture shorter-term dynamics of the whole system. A detached house located in London (UK) is selected as a case study, with the real hourly thermal load and electricity load profiles as well as hourly meteorological information, annual simulations are conducted to assess the techno-economic feasibility of the proposed micro-CHP system.

In the following sections, firstly the micro-CHP system is presented, along with the transient system model and the methods used for the energetic, economic and environmental assessments. This is followed by results concerning the effects of key component sizes and operating parameters, including collector flow rate, storage tank size, SE micro-CHP flow rate, and battery capacity, on the energetic, economic and environmental performance of the proposed system; optimum parameters and conditions are selected accordingly. The daily and monthly operating characteristics of the proposed micro-CHP system are then assessed, and the annual performance of the system is compared to that of a reference system (gas boiler plus grid electricity) as well as other, alternative solar-based systems. Finally, key conclusions are drawn from the results.

2. System configuration

A schematic diagram of the proposed micro-CHP system is shown in Fig. 1. The core components of this system include a PVT collector array, a stratified hot water storage tank, a SE micro-CHP unit, and a battery pack. Two pumped water circulation loops connect the hot water storage tank with the PVT collector array and the SE micro-CHP unit, respectively. Several lead–carbon battery units are connected with the PVT collectors and the SE micro-CHP unit electrically through an inverter, to store the electricity produced by the two power sources.

The electrical output of the system is used to satisfy the household electricity demand, and the system also connects with the grid, to export any excess electricity and to act as a backup supply of electricity when the generation is lower than the demand. It should be noted that the SE micro-CHP unit could be fuelled by biomass to make the proposed system achieve a complete renewable heat and electricity supply.

In this work, polycarbonate flat-box PVT collectors with 3 × 2 mm rectangular channels proposed by the authors' [6], are used to convert solar irradiation into heat and electricity. Compared to conventional copper sheet-and-tube PVT collectors, the polycarbonate flat-box PVT

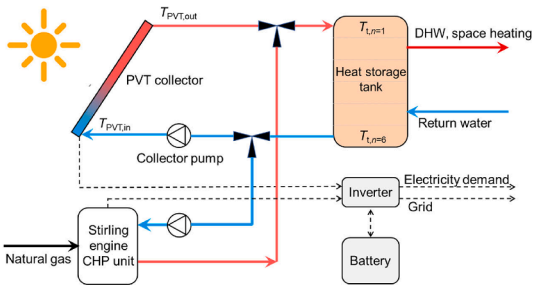

Fig. 1. Schematic diagram of the hybrid PVT collector, SE and energy storage system.

collectors have better thermal and economic performance. The aperture area and the nominal electric power output of each collector are 240 Wp and 1.55 m^2, respectively. Detailed technical specifications of the chosen collector are presented in Table 1.

The SE micro-CHP unit considered in this work is the Baxi Ecogen unit, which is the first widely available domestic SE micro-CHP product in the UK [33]. It is also one of the micro-CHP products certified by the Microgeneration Certification Scheme (MCS) of the UK and is eligible for the Smart Export Guarantee (SEG) scheme [34]. Fig. 2 shows a simplified layout of the SE micro-CHP unit considered in this work. It is a wall-mountable natural gas-fuelled SE-based boiler, and its core component is a free-piston Stirling engine (FPSE) manufactured by Microgen. The Baxi Ecogen unit has two burners, i.e., the main burner and the auxiliary burner (AB). The main burner is used for heating the head of the FPSE, and the FPSE then converts the combustion heat into mechanical work, which is further converted into electricity by a built-in linear alternator. The AB only operates when the heating demand is higher than the capacity of the main burner. Water flows into the unit and first flows through the FPSE cold-end heat exchanger and recovers heat from the engine. Then, it flows through the auxiliary heat exchanger and recovers heat from the exhaust gas. Afterwards, the water enters the heat exchanger of the AB, where its temperature can be further increased if necessary before it is pumped to the heating circuit. The Baxi Ecogen unit has an electrical capacity of 1.0 kW_e and a thermal capacity of 7.7 kW_{th}, and its thermal capacity can be boosted to 24 kW_{th} with the AB [36]. Detailed technical specifications of the unit are presented in Table 2.

The lead–carbon batteries are used to store or release electricity, and were selected based on their lower cost, compared to lithium-ion, flow, and sodium-sulphur batteries [37], and better performance than conventional lead-acid batteries.

3. Modelling and assessment methodology

A transient model of the proposed micro-CHP system was developed in the TRNSYS dynamic simulation software environment, using a simulation time step of 2 min, aimed at assessing the techno-economic performance of the system. The capital cost, replacement costs, operation costs, government incentives, and key economic and environmental parameters were all considered in these assessments. Here, key results are prenseted and discussed, and also compared to a reference system, which includes the electric grid based on the centralised natural gas power plant and a natural gas-fuelled boiler, as well as alternative solar-based cogeneration systems.

3.1. PVT collector

As mentioned above, the selected case study is a detached house in London, with an available roof area of around 29.5 m^2 for the installation of solar systems. The appropriate number of PVT panels is 18 according to the Solar Energy Calculator Sizing Guide from the UK Energy Saving Trust [38]. In simulations, the collector tilt angle is fixed at 38° [42]. It is optimised for maximum annual solar irradiation at London by using the Photovoltaic Geographical Information System (PVGIS) online tool [39]. The PVT collectors are modelled with a modified Type 560 in TRNSYS, which had been validated with experimental data, to match the

Table 1
Main technical specifications of the polycarbonate flat-box PVT collector [6,10].

Parameter	Value
Aperture area	1.55 m^2
PV cell type	Multi-crystalline silicon
Nominal output power	240 Wp
Nominal electrical efficiency	14.7%
Temperature coefficient of the PV cells	0.45%/K

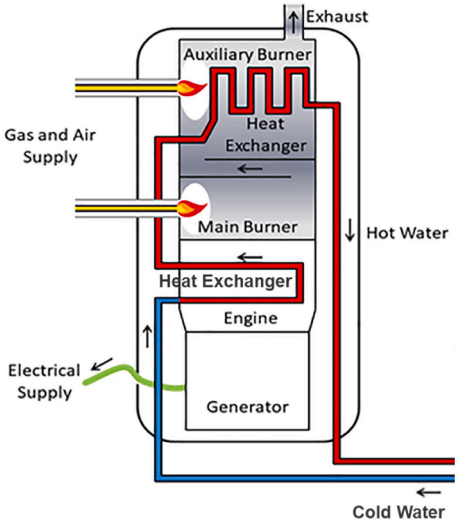

Fig. 2. Simplified layout of the considered SE micro-CHP unit [35].

Table 2
Main technical specifications of the Baxi Ecogen unit [36].

Specification	Value
Engine electrical capacity	0.3–1.0 kW_e
Engine thermal capacity	3.7–7.7 kW_{th}
Total thermal capacity (including AB)	24 kW_{th}
Electric efficiency	13%
Thermal efficiency	77%
Overall efficiency	90%
Dimensions	950 h × 450w × 420d (mm)
Noise	45 dB(A)
Weight	110 kg
Expected lifetime	10–15 years

thermal efficiency in Eqs. (1) and (2) [6]:

$$\eta_{th} = \frac{q_u}{G_T} = 0.726 - 3.325 \bullet T_r - 0.0176 \bullet G_T \bullet T_r^2 \quad (1)$$

$$T_r = \frac{T_{fm} - T_a}{G_T} \quad (2)$$

where q_u and G_T are the useful heat flow and global solar irradiance on the module plane; and T_r, T_{fm}, and T_a are the reduced temperature, mean fluid temperature and ambient temperature.

For the electrical performance, the modified Type 560 correlates PV efficiency (η_{PV}) linearly to the cell temperature (T_{PV}) and the global solar irradiance (G_T) [10]:

$$\eta_{PV} = \eta_{ref}[1 - \beta_r(T_{PV} - T_{ref})][1 + \beta_G(G_T - G_{ref})] \quad (3)$$

where η_{ref}, T_{ref} and G_{ref} are the electrical efficiency, cell temperature and incident irradiance respectively, at reference conditions, i.e., η_{ref} = 14.7 %, G_{ref} = 1000 W/m^2, and T_{ref} = 25 ℃; and β_r and β_G are the temperature coefficient and incident radiation coefficient of the solar cell.

3.2. SE micro-CHP unit

In order to simulate the performance of the Baxi Ecogen unit, a dynamic sub-model for the SE micro-CHP unit is developed and implemented into the TRNSYS simulation environment as a self-tailored Type 159. With the objectives of predicting fuel consumption and electric and thermal production accurately, the sub-model is developed by using a grey-box modelling approach and considers the dynamics that occur during the four different operation modes: stand-by, warming-up, full-

load operation, and shutting-down. In addition, the partial load performance of the SE is also considered in the sub-model. Specifically, the sub-model adopts general mass and energy conservation principles with support from empirical expressions for parametric factors obtained from experiments. Fig. 3 shows the mass and energy flows of the SE micro-CHP sub-model. The sub-model set out three control volumes (including the main burner, the heat exchanger and the AB block) and a control mass (i.e., the engine block) to simulate the dynamic thermal performance of the micro-CHP unit. The developed sub-model is validated with experimental data under both steady-state and dynamic working conditions, and good agreements between the numerical and experimental results have been obtained. More details of the sub-model and the validation can be found in Refs. [35] and [40].

3.3. Hot water storage tank

A stratified fluid storage tank model (Type 4 in TRNSYS) is used to simulate the hot water storage tank. In this model, the thermal stratification effects are considered by assuming that the storage tank consists of N ($N \leq 100$) equal volume segments along its vertical axis. The degree of stratification is determined by the value of N. For N equals 1 means no stratification effects are considered. The energy balance equation is set up for each volume segment respectively, and the temperatures of the N segments as functions of time can be obtained by solving these equations. More mathematical details about Type 4 can be found in Ref. [41]. In this work, the value of N is set to be 6 [10]. In addition, the storage tank diameter is fixed at 1 m, and its volume is varied by changing its height [42]. The hot water delivery temperature from the tank is set to be 60 ℃, with a return temperature of 40 ℃ [42].

3.4. Rest of the system

The inverter is modelled using an inverter/charge controller module (Type 48) in TRNSYS. The inverter efficiency and regulator efficiency are set to be 0.96 and 0.89, respectively. In addition, the electrical storage unit is modelled with a battery bank module (Type 47) in TRNSYS, and the charging efficiency is defined as 0.9. The dispatch strategy for electricity is as follows: the priority for the SE and PVT collector electric outputs are always to meet the load; when the electricity generated by the two power sources is greater than the load demand, the excess electricity will be used to charge the battery; once the state-of-charge (SoC) of the battery reaches the high limit value, the remaining electricity will be exported to the grid. The other way around, when the electricity generated by the two power sources cannot meet the load demand, the battery will discharge to cover the gap between the demand and the supply; once the SoC of the battery reaches the low limit value, the electricity deficit will be filled entirely by importing electricity from the grid. The hourly thermal energy and electricity demand profiles are read by a data reader module (Type 9) respectively, and these demand profiles are interpolated as two-minutely demand profiles for the simulations. A weather data processor module (Type 15) is used to read and interpret the meteorological data of London. Two constant speed pump modules (Type 114) are used to model the two pumps for the PVT collector water circulation loop and the SE micro-CHP water circulation loop, respectively.

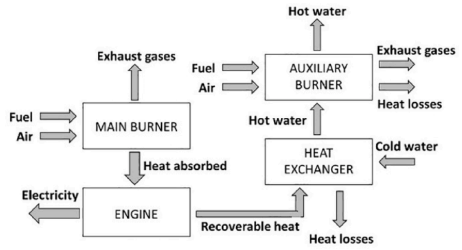

Fig. 3. Mass and energy flows of the sub-model for the SE micro-CHP unit [35].

A differential temperature controller (Type 2b) controls the operation of the collector pump by comparing the water temperature at the top of the storage tank ($T_{t,n=1}$) with the water temperature at the PVT collector outlet ($T_{PVT,out}$). To avoid the collector pump to be switched on and off frequently, the collector pump is switched on and the water from the PVT collector is sent to the water storage tank when the temperature difference ($T_{PVT,out} - T_{t,n=1}$) is higher than a minimum set-point value ΔT_{on}^{PVT}; when the temperature difference drops lower than a minimum set-point value ΔT_{off}^{PVT}, the collector pump is switched off and the water from the PVT collector does not circulate to the tank. In this work, ΔT_{on}^{PVT} and ΔT_{off}^{PVT} are chosen as 5 ℃ and 0.5 ℃, respectively, according to the recommended values from most domestic installations [42].

The control target of the SE micro-CHP unit is to maintain the supply water temperature above a certain value. To achieve this, another identical differential temperature controller (Type 2b) controls the operation of the SE micro-CHP unit by comparing the water temperature at the top of the storage tank, $T_{t,n=1}$, with a preset water temperature of 65 ℃ (T_{preset}^{SE}). Similarly, to avoid the SE micro-CHP unit to be switched on and off frequently, the SE micro-CHP unit (here means the main burner) is switched on and the heated water from the SE micro-CHP unit is sent to the water storage tank when the temperature difference ($T_{preset}^{SE} - T_{t,n=1}$) is higher than a minimum set-point value ΔT_{on}^{SE}, when the temperature difference drops lower than a minimum set-point value ΔT_{off}^{SE}, the SE micro-CHP unit is shut down. In this work, ΔT_{on}^{SE} and ΔT_{off}^{SE} are set to be 5 ℃ and 0 ℃, respectively. The operation of the AB is also controlled by a differential temperature controller (Type 2b), which compares $T_{t,n=1}$ with a preset water temperature of 62 ℃ (T_{preset}^{AB}). The AB of the SE micro-CHP unit is switched on when the temperature difference ($T_{preset}^{AB} - T_{t,n=1}$) is higher than a minimum set-point value ΔT_{on}^{AB}, when the temperature difference drops lower than a minimum set-point value ΔT_{off}^{AB}, the AB is shut down. In this work, ΔT_{on}^{AB} and ΔT_{off}^{AB} are chosen as 3 ℃ and 0 ℃. Therefore, in this work, when $T_{t,n=1}$ is below 59 ℃, both the main burner and the AB will be switched on, and when $T_{t,n=1}$ is lifted above 62 ℃ but lower than 65 ℃, the AB will be shut down and the main burner will remain working. When $T_{t,n=1}$ is lifted above 65 ℃, the main burner will be switched off.

The model of the proposed micro-CHP system developed in TRNSYS includes three main sub-models (referred to as 'Types'), the PVT collector sub-model (Type 560), the SE micro-CHP unit sub-model (self-tailored Type 159), and the hot water storage tank sub-model (Type 4). For the PVT collector sub-model (Type 560), the deviations between the simulated values (including heat and electricity production and efficiency) from the measured values are within 13% [43]. For the SE micro-CHP unit sub-model, the deviations between the simulated values (including fuel input and the heat and electricity outputs) from the measured values are within 10% [35]. The hot water storage tank sub-model used in this work (i.e., Type 4) is an extensively used model for storage tank modelling in TRNSYS, whose accuracy has been widely validated [44,45]. Therefore, all three sub-models are sufficiently accurate to provide meaningful system-level results, and ensure the credibility of the results presented in this work.

3.5. Building energy demands

A detached house in the Milton Keynes residential community in north London (UK) is chosen for the techno-economic performance evaluation of the proposed system. The floor area of the house is 136.1 m^2, with 4 bedrooms and a maximum occupancy of 6. Hourly natural gas and electricity usage profiles of the selected house have been recorded, and complete one-year usage profiles are taken from the UK Energy Research Centre Energy Data Centre [46]. Assuming a constant boiler efficiency of 85% [47,48], the hourly natural gas usage profile is converted into a heat demand (including DHW and SP) profile. Then,

both the heat and electricity demand profiles are input to the developed model of the micro-CHP system. Fig. 4 shows the accumulated monthly heat and electricity demands. According to the recorded data, the annual heat demand of the selected house is 22.0 MWh, and the annual electricity demand is 4.65 MWh.

3.6. Energy analysis

To estimate the energy performance of the proposed micro-CHP system, some energy performance indexes have been defined. The household electricity self-sufficiency (ESS) is:

$$\mathrm{ESS} = \frac{E_{\mathrm{supply}}}{E_{\mathrm{demand}}} \tag{4}$$

where E_{supply} is the onsite use of electricity, which can be formulated as: $E_{\mathrm{supply}} = E_{\mathrm{demand}} - E_{\mathrm{import}}$, E_{demand} and E_{import} are the demand and imported electricity in the analysed time.

The thermal energy self-sufficiency (TSS, or thermal energy demand coverage) is defined as the ratio between the thermal energy production of the proposed system and the household thermal energy demand in the analysed time:

$$\mathrm{TSS} = \frac{Q_{\mathrm{supply}}}{Q_{\mathrm{demand}}} \tag{5}$$

where Q_{supply} and Q_{demand} denote the thermal energy supplied to heat loads from the water storage tank (i.e., the total thermal production from the SE micro-CHP unit and the PVT collector, which excludes the thermal loss of the water storage tank) and the thermal demand of the house.

The installation of micro-CHP systems can greatly reduce household primary energy consumption. To evaluate the degree of such benefit achievable with the proposed system, an indicator known as Primary Energy Saving (PES) is introduced:

$$\mathrm{PES} = 1 - \frac{G_{\mathrm{pro}}}{\frac{E_{\mathrm{pro}}}{RefE_{\eta}} + \frac{Q_{\mathrm{supply}}}{RefQ_{\eta}}} \tag{6}$$

where G_{pro} and E_{pro} are the gas consumption and electricity production of the proposed system, respectively, the latter is calculated as the sum of the onsite use of electricity (E_{supply}) and the exported electricity (E_{export}); $RefE_{\eta}$ and $RefQ_{\eta}$ are the efficiency for separate power and heat productions respectively, i.e., a gas boiler and grid electricity. In this study, efficiencies of 0.85 [47,48] and 0.48 [49] are assumed for the gas boiler and the national electric grid.

3.7. Economic analysis

An economic feasibility analysis for the system was conducted over a period of 30 years. This period is chosen according to the longest estimated lifetime of the system components: PVT collector,s which have an excepted lifetime of 25–30 years [50,51].

The net present value (NPV) and the payback period are used here to measure the economic feasibility of the proposed system. The NPV is calculated by using Eq. (7) [52]:

$$\mathrm{NPV} = -\mathrm{INV} + \sum_{n=1}^{n=30} \frac{CF_{\mathrm{n}}(1+i)^{n-1}}{(1+d)^{n}} \tag{7}$$

where i is the inflation rate, d is the discount rate, INV represents the additional initial investment for the proposed system in comparison with the reference system, and CF_n is the annual net saving in the nth year.

The employed initial investment data for different components are shown in Table 3, and the capital cost and specification of the battery cells being used in this study are given in Table 4. In addition, the annual net saving in the nth year, CF_n, is calculated by using Eq. (8):

$$CF_n = E_{\mathrm{ref},n}c_{\mathrm{e}} + G_{\mathrm{ref},n}c_{\mathrm{ng}} + M_{\mathrm{boiler},n} + R_{\mathrm{ref},n} - \left(E_{\mathrm{import},n}c_{\mathrm{e}} + G_{\mathrm{pro},n}c_{\mathrm{ng}} + M_{\mathrm{SECHP},n} + M_{\mathrm{PVT},n} + R_{\mathrm{pro},n} - E_{\mathrm{export},n}\mathrm{SEG}_{\mathrm{tariff}}\right) \tag{8}$$

where $E_{\mathrm{ref},n}$ and $G_{\mathrm{ref},n}$ are the gas consumption and electricity purchased from the grid for the reference system, respectively; c_{e} and c_{ng} are unit electricity and natural gas prices, respectively; $M_{\mathrm{boiler},n}$ is the annual maintenance cost of the gas boiler, which is estimated as £120/year [21]; $R_{\mathrm{ref},n}$ denotes the replacement cost for the reference system at year n (the lifespan of the gas boiler is assumed to be 15 years [33], so the gas boiler should be replaced at the end of year 15); $G_{\mathrm{pro},n}$ and $E_{\mathrm{import},n}$ are the gas consumption and electricity purchased from grid for the proposed system, respectively; $M_{\mathrm{SECHP},n}$ is the annual maintenance cost of the SE micro-CHP unit, which is estimated as £130/year [21]; $R_{\mathrm{pro},n}$ is the replacement cost for the proposed system at year n. In this study, the lifespan of the SE micro-CHP unit is assumed to be 15 years, so it should be replaced at the end of year 15. In addition, the expected lifespan for the inverter and battery cells is 15 years [53] and 10 years [21]. A summary of the expected lifespan and replacement cost for each component in the reference system and the proposed system is given in Table 5. In the UK, the SEG scheme, which is designed to ensure small-scale generators are paid for the renewable electricity they export to the grid [34], can be applied to the proposed system. It should be also noted that different energy companies offer different SEG tariffs [54]. In this work, the SEG tariff is assumed as £0.05/kWh based on the average tariff from energy companies [55]. In Eq. (8), the term $E_{\mathrm{export},n}\mathrm{SEG}_{\mathrm{tariff}}$ denotes earnings from exporting surplus electricity to the grid.

The payback period is defined here as the time needed for the cumulative annual net savings to become equal to the total initial investment, i.e., NPV = 0. The economic parameters used in the simulations are summarised in Table 6.

3.8. Environmental analysis

In order to estimate the potential environmental benefits of switching from a reference system to the proposed system, a carbon emission analysis was performed for both systems, to identify the extent to which the emissions are lower than those associated with the reference system. For the house fitted with the system, the quantity of carbon emissions is the carbon emissions associated with electricity imported from the grid

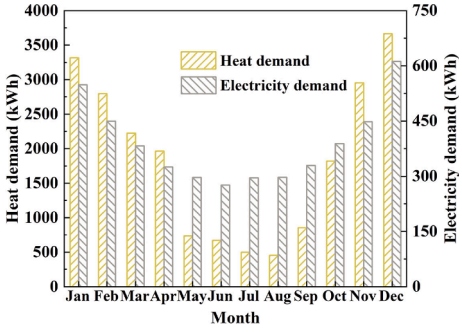

Fig. 4. Accumulated monthly heating and electricity demands.

Table 3
Cost breakdown of the micro-CHP system.

Component	Value	Unit	Source
SE micro-CHP unit (including AB)	7370	£/unit	[33]
PVT collector	260	£/collector	[42]
Pump station for PVT collector	203	£/unit	[56]
Mounting	51	£/collector	[42]
Inverter	545	£/unit	[57]
Water storage tank	0.752 V_{t}(L) + 656.6	£	[42]
Pipes (including insulation)	9.5	£/m	[42]
System installation	34	£/m^2	[10]

Table 4
Capital cost and specification of the battery cells [58].

Component	Specification	Cost (£)
Battery cells 1.3 kWh	12 V 106 Ah × 1	289
Battery cells 2.5 kWh	12 V 106 Ah × 2	578
Battery cells 3.8 kWh	12 V 106 Ah × 3	867
Battery cells 5.1 kWh	12 V 106 Ah × 4	1156
Battery cells 6.4 kWh	12 V 106 Ah × 5	1445
Battery cells 7.6 kWh	12 V 106 Ah × 6	1734
Battery cells 8.9 kWh	12 V 106 Ah × 7	2023
Battery cells 10.2 kWh	12 V 106 Ah × 8	2312

Table 5
Expected lifespan and replacement cost for each component.

Component	Lifespan (year)	Replacement cost (£)	Source
Inverter	15	545	[56]
SE micro-CHP unit	15	7370	[33]
Battery cells	10	See Table 4	See Table 4
Gas boiler	15	2500	[21]

Table 6
Economic parameters used in the simulations.

Parameter	Value	Source
Electricity purchase price, c_e	£0.213/kWh	[59]
Natural gas price, c_{ng}	£0.041/kWh	[60]
Discount rate, d	3.50%	[61]
Inflation rate, i	2.70%	[42]
PVT maintenance, M_{PVT}	1% of the investment cost	[2,62]
SE micro-CHP unit maintenance, M_{SECHP}	£130/year	[21]
SEG tariff, SEG_{tariff}	£0.05/kWh	[63]
Boiler maintenance, M_{boiler}	£120/year	[21]

plus the carbon emissions associated with gas consumption, and minus the avoided carbon emissions associated with electricity exported to the grid. The emitted carbon associated with the proposed system, EC_{pro}, is defined as:

$$EC_{pro} = E_{import,n} CI_{ge} + G_{pro,n} CI_{ng} - E_{export,n} CI_{ge} \quad (9)$$

where CI_{ge} and CI_{ng} denote carbon emission factors for grid electricity and natural gas, respectively. In this study, carbon emission factors for gas and electricity are selected as 0.184 $kgCO_{2\text{-}eq}$/kWh [42] and 0.4116 $kgCO_{2\text{-}eq}$/kWh [64], respectively.

For the house fitted with the gas boiler, the total quantity of carbon emissions, EC_{ref}, arises from component associated with the electricity imported from the grid plus a second component associated with the gas consumption, and can be expressed as:

$$EC_{ref} = E_{ref,n} CI_{ge} + G_{ref,n} CI_{ng} \quad (10)$$

In addition, the carbon emission reduction rate, ΔCO_2, is defined as the carbon emission reduction achieved by the proposed system relative to that of the reference system:

$$\Delta CO_2 = \frac{EC_{ref} - EC_{pro}}{EC_{ref}} \quad (11)$$

4. Results and discussion

4.1. Parametric sensitive analyses

For the given installation number of PVT collectors and household energy-demand data, the impact of key component sizes and operating parameters, including collector flow rate, storage tank size, SE micro-CHP flow rate and battery capacity on the energetic, economic and environmental performances of the proposed system are evaluated and analysed. To take the accumulative effect into account, these analyses are performed over an entire year of operation.

4.1.1. Effect of collector flow rate

According to Herrando et al. [65], the PVT collector flow rate affects significantly the thermal and electrical production performance of a standalone PVT system. The authors of this study concluded that the heating demand covered by a standalone PVT system is considerably more sensitive than the electrical demand covered to the increase in PVT collector flow rate. However, how the PVT collector flow rate impacts the system's energy performance, and further the economic and environmental performances is unclear. As such, collector flow rates ranging from zero (no water flow through the collector, in this condition, and the PVT collectors can be regarded as PV panels) to 200 kg/h, with higher resolution in the range 0–35 kg/h, are studied. To rule out the influence of the storage tank size and battery capacity, the storage tank size and battery capacity are set to be 840 L and 5 kWh, respectively.

Fig. 5(a) shows the effect of the PVT collector flow rate on the generated and imported electricity (for the generated electricity herein, the loss caused by electricity management is not considered). When the PVT collector flow rate increases from 0 to 20 kg/h, there is a remarkable increase (from 3000 to 3260 kWh, increased by 8.5%) in the annual electricity generated by the PVT collectors. This is because, during the operation of the system, the PV module temperature is reduced by the circulation water, which allows a higher PV module efficiency. At lower collector flow rates, the growth of the collector flow rate will lead to an increase in PV efficiency. Hence the annual electricity generated by the PVT collectors increases with the growth of the collector flow rate. However, with a further increase in the collector flow rate, the PV efficiency is not further enhanced and approaches a saturation value, and the annual electricity generated by the PVT collectors almost keeps constant at around 3260 kWh (It should be noted the electricity consumed by the collector pump is not considered herein, and it is anticipated that the net generated electricity by the PVT collectors will decrease slightly at a higher collector flow rate due to the more electricity consumed by the collector pump). As in a standalone PVT system, the thermal output of the PVT collectors is more sensitive than the electrical output to the increase in the PVT collector flow rate. As shown in Fig. 5(c), when the PVT collector flow rate increases from 0 to 20 kg/h, the heat transferred to the water flowing through the PVT collector increases, and the annual heat production improves from 0 to 4510 kWh; with a further increase in collector flow rate, the annual heat production of the PVT collectors declines slightly. This is mainly because, at high flow rates, the water temperature at the outlet from the collectors is low, the water from the collectors cannot be used to heat the storage tank, and the running time of the collector heating water circulation loop (i.e., the running time of the collector pump) decreases accordingly (as shown in Fig. 5(d)), leading to a decrease in the annual heat production.

When there is no water flow through the PVT collector, the household thermal demand is satisfied only by the SE micro-CHP unit, which requires the annual running times of the SE and the AB to be considerably long, as shown in Fig. 5(d). Therefore, the annual electricity generated by the SE at a collector flow rate of zero is the highest among the studied collector flow rates (see Fig. 5(a)). When the PVT collector flow rate increases from 0 to 20 kg/h, the annual electricity generated by the SE drops obviously (from 3610 to 2820 kWh, reduced by 22%) due to the reduction in running time. This makes the total annual electricity generated by the two generators decrease, and the annual imported electricity increases accordingly. Therefore, as shown in Fig. 5(b), the EES decreases with the increase of the collector flow rate when the collector flow rate is below 20 kg/h. When the flow rate is higher than 20 kg/h, the EES almost keeps constant at 87%. In contrast to the EES, the fluctuation of the TSS is quite small, it maintains above 99% for all the studied collector flow rates (see Fig. 5(c)). As such, we can conclude that the collector flow rate does not influence the thermal output of the micro-CHP system strongly, but it does affect the electrical output.

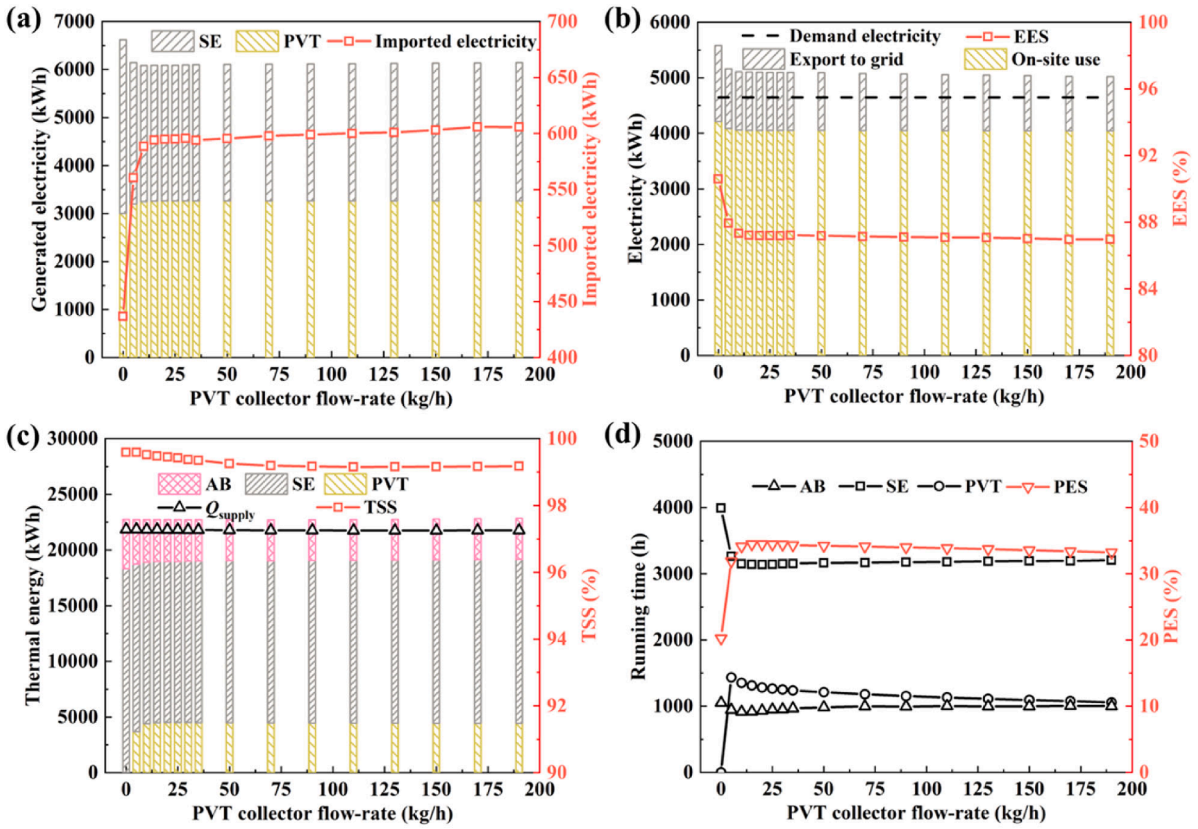

Fig. 5. (a) Generated and imported electricity, (b) electricity distribution and EES, (c) thermal energy production and TSS, and (d) different heating approach running times and PES of the proposed CHP system, with different collector flow rates.

With the introduction of the PVT collector, the benefit of a PVT collector-based system compared to a PV-based system [21] is obvious, as proven in the PES variation curve shown in Fig. 5(d). The PES climbs from 20% to 34% when the PVT collector flow rate increases from 0 to 20 kg/h. This is mainly because of the extra thermal production of the PVT collectors and the enhancement in electrical production in comparison with PV panels. Correspondingly, both the economic and environmental benefits are improved significantly when the PVT collector flow rate increases from 0 to 20 kg/h, as shown in Fig. 6(a) to 6(b). A maximum NPV of £1990 is achieved at a PVT collector flow rate of 20 kg/h, corresponding to a payback period of 28 years, hence the PVT collector flow rate is selected as 20 kg/h for the proposed system. Further increase in the PVT collector flow rate will decrease the NPV of the proposed system to some extent. This is mainly because of the increase in the electricity consumed by the PVT collector pump and the decrease in heat production from the PVT collectors, with large collector flow rates. Meanwhile, with a PVT collector flow rate of 20 kg/h, the proposed system has the potential to displace around 2.47 tons of CO_2 relative to the reference system over a year, corresponding to a reduction rate of 37%. By comparison, PV-based solution displaces 1.57 tons CO_2/year with a reduction rate of 24% from the same installation area.

4.1.2. *Effect of storage tank size*

In a single CHP system, for a given thermal demand profile and CHP prime mover thermal power size, the size of the thermal storage system has a strong influence on the operating time of the prime mover [66],

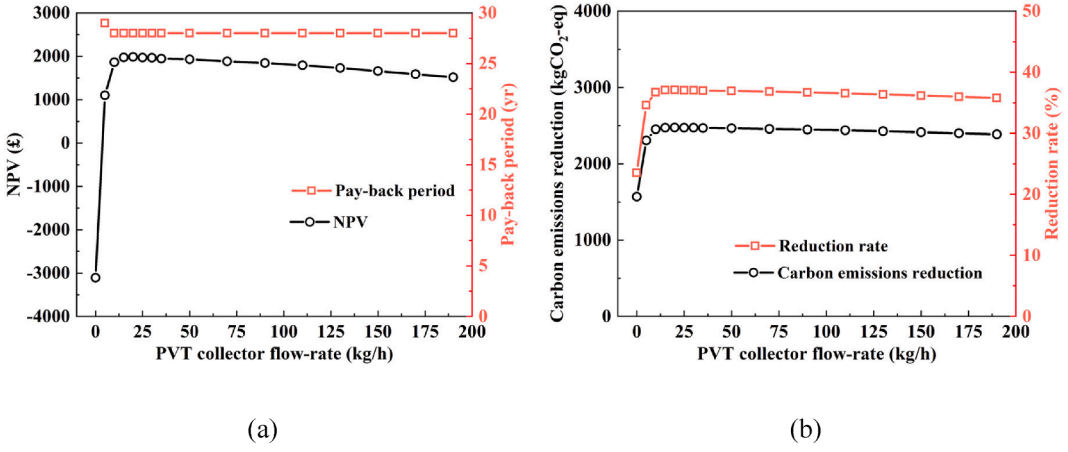

Fig. 6. (a) NPV and payback period, and (b) annual carbon emission reduction and reduction rate of the proposed system, with different collector flow rates.

which will further influence the heat and electricity generation of the CHP system, as well as the economic performance and environmental performance [67,68]. For the proposed system, the situation will be more complex since the two prime movers operate synergistically. To explore the effect of the storage tank size on the micro-CHP system performance, a commonly used ratio in solar thermal systems [42], V_t/A_{cT}, is employed herein to perform the analysis (V_t is the storage tank volume in litre and A_{cT} is the total PVT collector array area, here is 27.9 m^2). In the analysis, the ratio V_t/A_{cT} is varied from 2.5 to 100 L/m^2, i.e., the storage tank volume varies from 69.8 to 2790 L. Meanwhile, the PVT collector flow rate and battery capacity are selected as 20 kg/h and 5 kWh, respectively.

Fig. 7(a) and 7(b) present the influence of storage tank size on the electrical output performance of the micro-CHP system. In contrast to the collector flow rate, the storage tank size does not notably influence the electricity generation by the PVT collectors. With the increase of V_t/A_{cT} from 2.5 to 100 L/m^2, the storage tank volume is increased by 39 times, while the annual electricity generation by the PVT collectors is only improved by 6.3%. The slight improvement in annual electricity generation arises from the increase in the operating time of the collector heating water circulation loop (as shown in Fig. 7(d)), which increases the operating time of the PV panels at lower operating temperatures to some extent. The operating time of the SE is more sensitive to the V_t/A_{cT} in comparison to that of the collector heating water circulation loop, and it first decreases and then increases with the growth of V_t/A_{cT}. The shortest operating time of the SE, 3130 h, is obtained at a V_t/A_{cT} of 50 L/m^2. The variation of the annual electricity generation by the SE is strongly related to the operating hours of the engine, which makes the variation of the EES of the system similar to that of the annual electricity generation by the SE, while achieving a minimum value at a larger V_t/A_{cT} (70 L/m^2), as shown in Fig. 7(b).

For the thermal output of the micro-CHP system, with the growth of V_t/A_{cT}, the annual thermal energy generation by the PVT collectors increases gradually, with a decreasing slope. For the annual thermal energy generation by the SE, its variation trend is similar to that of the operating time of the SE. This can be explained as follows: at very low V_t/A_{cT}, the thermal energy storage capacity of the storage tank is rather low, to meet the given heat demand, the only solution is to increase the operating time of the SE and the AB. As the value of V_t/A_{cT} increases, more generated thermal energy can be stored in the tank, which could reduce the operating time of the SE and the AB to some extent. However, at high V_t/A_{cT}, due to the large thermal mass in the tank and the considerable heat loss (the difference between the total thermal energy generation by the SE, PVT and AB, and the supplied thermal energy by the system, as shown in Fig. 7(c)), the temperatures throughout the tank are lower. Though this will increase the operating time of the collector heating water circulation loop and the thermal energy generation by the PVT collector, extra thermal energy from the SE is still required to reach the pre-set temperature of supply water. As shown in Fig. 7(c), the TSS of the proposed micro-CHP system maintains above 99%, with the variation of V_t/A_{cT}. This is quite different from that of a standalone PVT system [42], and it can be attributed to the synergy between these three heating approaches. In addition, the annual PES of the system increases slightly with the growth of V_t/A_{cT} when V_t/A_{cT} is smaller than 40 L/m^2, and later it almost keeps constant at 35%.

Fig. 8(a) presents the effect of V_t/A_{cT} on the NPV and payback period of the micro-CHP system. Generally, a decrease in SE operating time and an increase in the operating time of the PVT collector heating water circulation loop will enhance the annual net saving of the system. Therefore, the NPV first increases with the growth of V_t/A_{cT} when V_t/A_{cT} is less than 20 L/m^2. However, with further increase in V_t/A_{cT}, the capital cost of the storage tank increases significantly, which makes the INV of the system rise accordingly. Hence, the NPV declines gradually after reaching a peak value in 2000 £ at a V_t/A_{cT} of 20 L/m^2. Conversely, the shortest payback period of 28 years is achieved in the V_t/A_{cT} range of 10–50 L/m^2. As for the effect of V_t/A_{cT} on the potential environmental

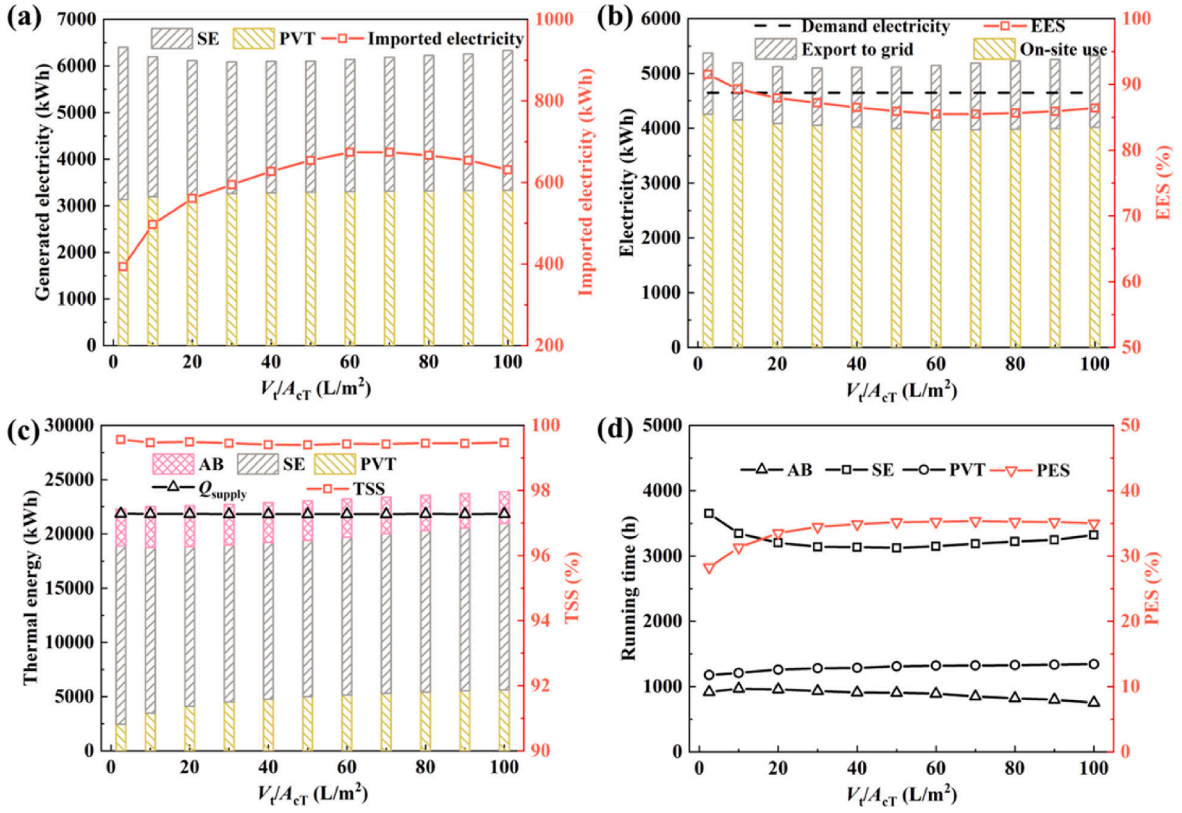

Fig. 7. (a) Generated and imported electricity, (b) electricity distribution and EES, (c) thermal energy production and TSS, and (d) different heating approach running times and PES of the proposed system, with different V_t/A_{cT} ratios.

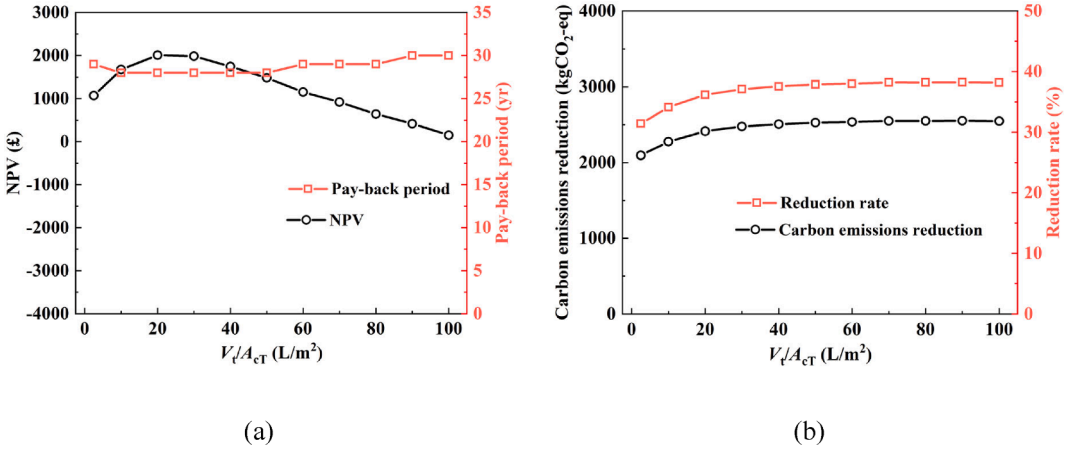

Fig. 8. (a) NPV and payback period, and (b) annual carbon emission reduction and reduction rate of the proposed system, with different V_t/A_{cT} ratios.

benefits of the system, both the annual carbon emission reduction amount and the carbon emission reduction rate increase with the lift of the thermal energy storage capacity of the system, while with a reducing slope, as shown in Fig. 8(b). Therefore, an 840 L storage tank volume is selected (i.e., a V_t/A_{cT} of 30 L/m^2) for the proposed micro-CHP system as a compromise value between the NPV and environmental benefits.

4.1.3. *Effect of SE micro-CHP water flow rate*

For a standalone SE micro-CHP unit, the water flow rate of the unit has a significant influence on the electrical and thermal productions of the unit. Generally, in a steady state, for a given inlet water temperature, the higher the water flow rate, the more electrical and thermal power that the SE micro-CHP unit can produce [69]. In transient states, the effects of water flow rate on the transient electrical and thermal power of the SE micro-CHP unit are more complicated. To evaluate the effect of SE micro-CHP unit water flow rate on the micro-CHP system's annual performance, a series of water flow rates ranging from 300 to 900 kg/h are considered in this work.

Fig. 9(a) and 9(b) show the impact of SE micro-CHP unit water flow rate on the annual electrical production and distribution of the system. With the growth of the SE micro-CHP unit water flow rate from 300 to 900 kg/h, there is a slight decrease in annual electrical production by the SE (it decreases from 3020 to 2670 kWh by 11.6%), which is mainly caused by the reduction of the annual running time of the SE, as presented in Fig. 9(d). The reason for the reduction of the SE annual running time can be explained as follows: like a standalone SE micro-CHP unit, the greater the water flow rate, the lower the water temperature being lifted by the cold-end heat exchanger of the SE, leading to an increase in the operating time of the AB (to reach 62 °C at the top of the storage tank, i.e., the shutdown temperature for the AB), thus a longer operating

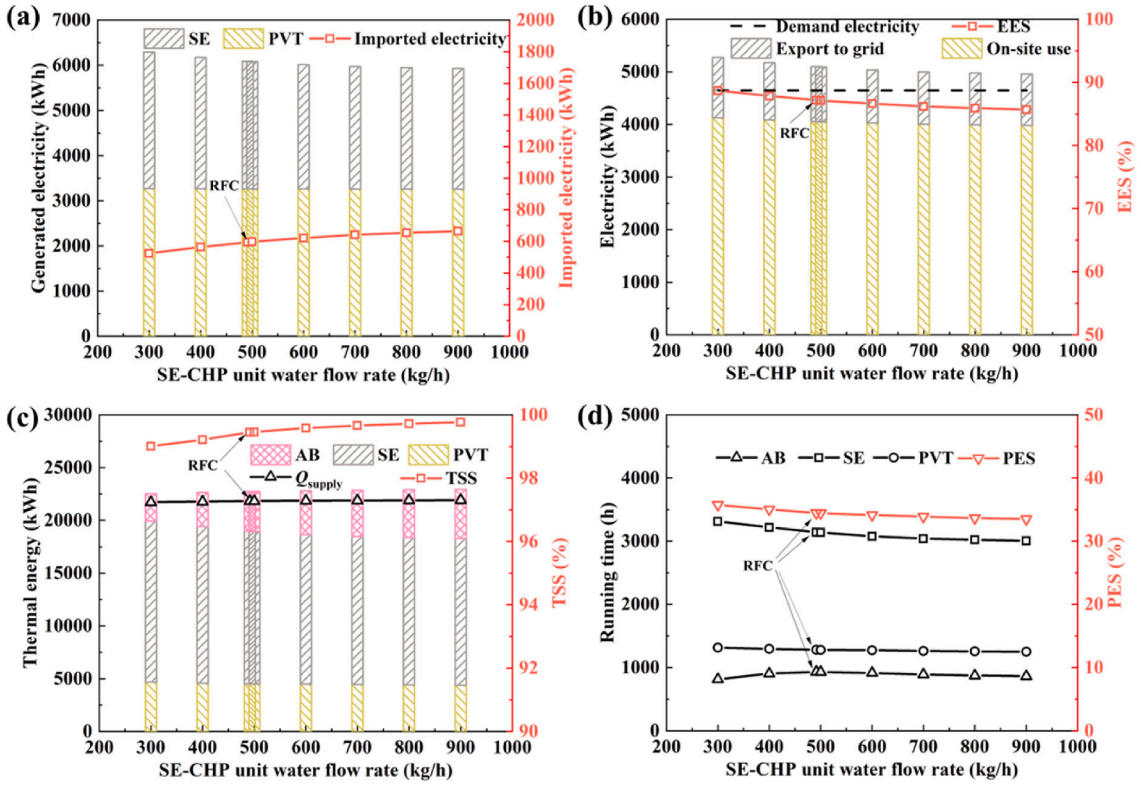

Fig. 9. (a) Generated and imported electricity, (b) electricity distribution and EES, (c) thermal energy production and TSS, and (d) different heating approach running times and PES of the proposed CHP system, with different SE micro-CHP unit water flow rates (RFC: reference flow conditions).

time for the SE is no longer required. In addition, the EES of the proposed system also declines with the growth of the SE micro-CHP unit water flow rate, since more imported electricity is required at a high water flow rate (read hollow squares in Fig. 9(a)). However, the variation trend of the TSS is quite different from that of the EES, as shown in Fig. 9 (c), the TSS increases with the growth of the SE micro-CHP unit water flow rate. The reason behind this is the annual heat production of the AB declines slightly due to the higher outlet water temperature at the cold-end heat exchanger at a lower water flow rate. Different from the influence of collector flow rate on the operation of SE, the SE micro-CHP unit water flow rate has a minor influence on the operation of the PVT collectors. The annual thermal and electrical productions of the PVT collectors almost keep constant with the change in SE micro-CHP unit water flow rate.

Fig. 10 (a) shows the effect of SE micro-CHP unit water flow rate on the NPV and payback period of the CHP system. One can conclude that lower water flow rates are beneficial for the increase in NPV and the reduction in the payback period, since more electricity is generated from the SE and the PVT collectors at lower water flow rates. Meanwhile, both the annual carbon emission reduction amount and the carbon emission reduction rate decrease with the growth of SE micro-CHP unit water flow rate.

4.1.4. *Effect of battery capacity*

As previously mentioned, the integration of electricity storage into a renewable energy system would reduce the variability of household grid demand, thus mitigating grid balancing issues to some extent. Though numerous studies have been performed to evaluate the influence of battery capacity on the operation of renewable energy systems [70,71], few analyses on such a micro-CHP system can be found in literature [21], in particular using a dynamic modelling approach to perform the analysis. As such, with the developed transient model, herein we considered different battery capacities ranging from 0 to 10.2 kWh (see Table 4) to reveal the effects of the battery capacity on the performance of the system. In the analyse process, the PVT collector flow rate and storage tank volume are selected at 20 kg/h and 840 L, respectively. Meanwhile, the SE micro-CHP unit water flow rate is fixed at the reference flow conditions, i.e., 490 kg/h.

Fig. 11(a) and 11(b) show the impact of battery capacity on the annual electrical production and distribution of the system. As expected, the battery capacity has no influence on the annual electrical productions of the SE and the PVT collectors. However, it has a strong influence on imported electricity and exported electricity. When the battery capacity increases from 0 to 5 kWh, the imported electricity declines from 1950 to 600 kWh (by 69%), while the exported electricity reduces from 2610 to 1050 kWh (by 60%), making the EES rise from 58% to 87%. However, with further increases in the battery capacity, the reductions in both imports and exports are marginal, which is consistent with the results reported in Ref. [21]. The battery capacity also has no influence on the annual running time and heat production of the SE, the PVT collectors, and the AB, as shown in Fig. 11 (c) and 11(d).

Fig. 12(a) shows the dependence of the system NPV and payback period on the battery capacity. Generally, when the electricity export price is lower than the electricity import price, avoiding electricity export and reducing electricity import by increasing the battery capacity leads to financial benefits. Hence the NPV increases with the growth of battery capacity at smaller battery capacities. However, when the battery capacity is larger than 5 kWh, the NPV declines with the growth of battery capacity. This is mainly because, with larger battery capacities, the capital and equipment replacement costs are more considerable, which cannot be nullified by the financial benefit obtained by increasing the battery capacity. Given the NPV of the proposed system with a 5 kWh battery is higher than that of the proposed system with other battery capacities, a battery capacity of 5 kWh is selected. Fig. 12(b) shows the annual carbon emission reduction and reduction rate of the system versus battery capacity. Since with the growth of battery capacity, the difference between the exported electricity and the imported electricity decreases, as per Eq. (9), both the annual carbon emission reduction and reduction rate of the proposed system decline accordingly.

4.2. *Operating characteristics of the proposed micro-CHP system*

From the parametric sensitive analysis results shown above, we finally choose the PVT collector flow rate, storage tank volume, SE micro-CHP unit water flow rate, and battery capacity as 20 kg/h, 840 L, 490 kg/h, and 5 kWh, respectively, by compromising the NPV and the environmental benefits of the proposed micro-CHP system. Based on the determined system sizes and operating parameters, the daily and monthly operating characteristics of the proposed system are evaluated, and the annual performance of the proposed system is compared to that of the reference system as well as other, alternative solar-based systems. Finally, the influence of utility (electricity, natural gas) prices on the system's economics is evaluated.

4.2.1. *Daily operating characteristics*

Fig. 13 shows the generated and supplied thermal power of the proposed system along with the heat demand profile and solar irradiance during the four typical days that represent the four seasons of a year. As shown in Fig. 13(a) to 13(d), the effects of solar irradiance on the heat generation of the PVT collectors are evident. For example, both the running time of the collector heating water circulation loop and the heat generation by the PVT collectors in summer is much larger than

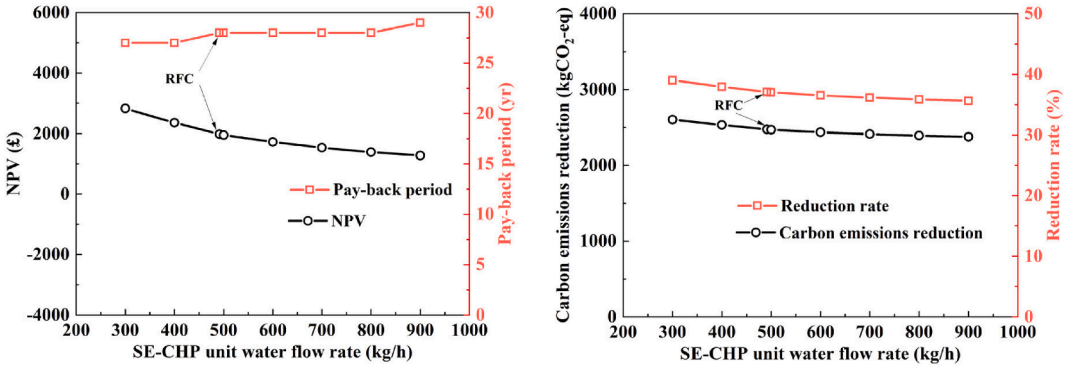

Fig. 10. (a) NPV and payback period, and (b) annual carbon emission reduction and reduction rate of the proposed system, with different SE micro-CHP unit water flow rates.

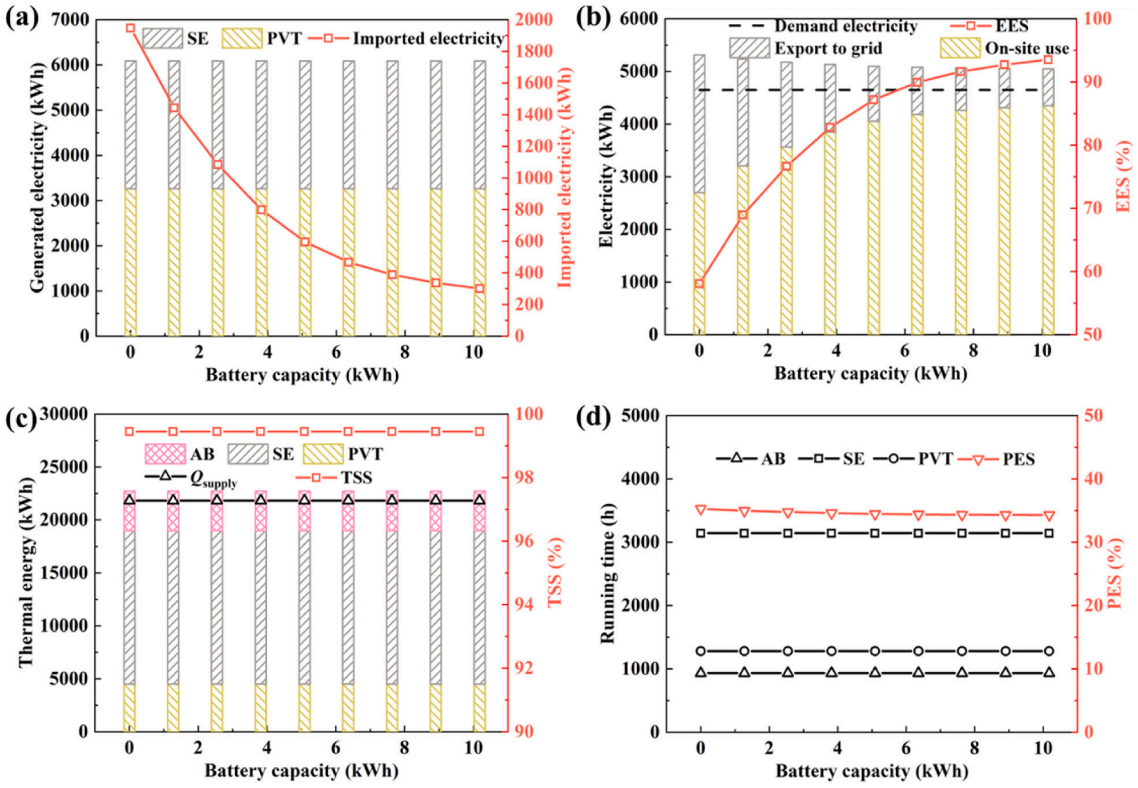

Fig. 11. (a) Generated and imported electricity, (b) electricity distribution and EES, (c) thermal energy production and TSS, and (d) different heating approach running times and PES of the proposed system, with different battery capacities.

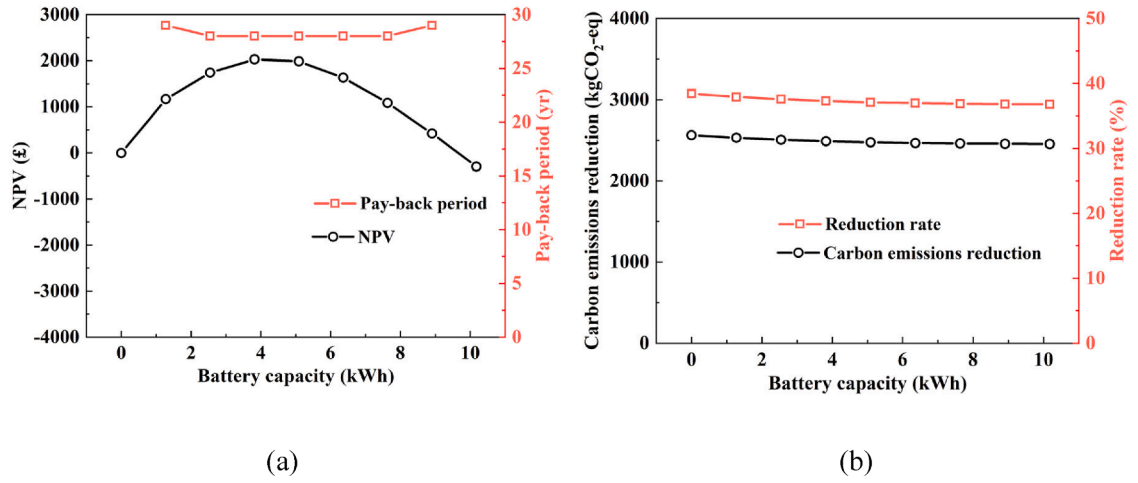

Fig. 12. (a) NPV and payback period, and (b) annual carbon emission reduction and reduction rate of the proposed system, with different battery capacities.

that of in winter and autumn, and on the chosen typical day in spring, the PVT collectors even cannot generate useful heat due to the low solar irradiance. Moreover, since there is a smaller household heat demand while the PVT heat output is quite large in summer, both the SE and the AB are unused during the day in summer. The opposite is true in the winter and autumn, the operating hours of the AB and SE are prolonged due to the low PVT heat output and large household heat demand. It is also interesting to see that the heat generation of the SE micro-CHP unit matches well with the heat demand. However, there is a mismatch between the PVT heat generation and heat demand, especially in summer. For example, in summer, the PVT heat generation mainly occurs between 8:00 am and 15:00 pm, while the peak heat demand concentrates between 16:00 pm and 19:00 pm. However, with the thermal buffer effect provided by the thermal storage system, the heat supply profiles coincide well with the heat demand profiles on all four typical days.

As for the daily electricity generation and distribution on the four typical days, as shown in Fig. 14(a) to 14(d), the variation of PVT electricity generation on the four different typical days presents the same characteristics as the variation of PVT heat generation, due to the variation in solar irradiance. For example, on 21st June, the output electric power generated by the PVT is greater than the energy required by the load since 6:00 am, the control dispatch strategy of the proposed system will match the electrical demand first and the remaining energy is used to charge the battery (the positive section of the yellow curve in Fig. 14(b)). When the SoC of the battery reaches the high limit value since the time of 12:30 pm, the battery is unable to store additional

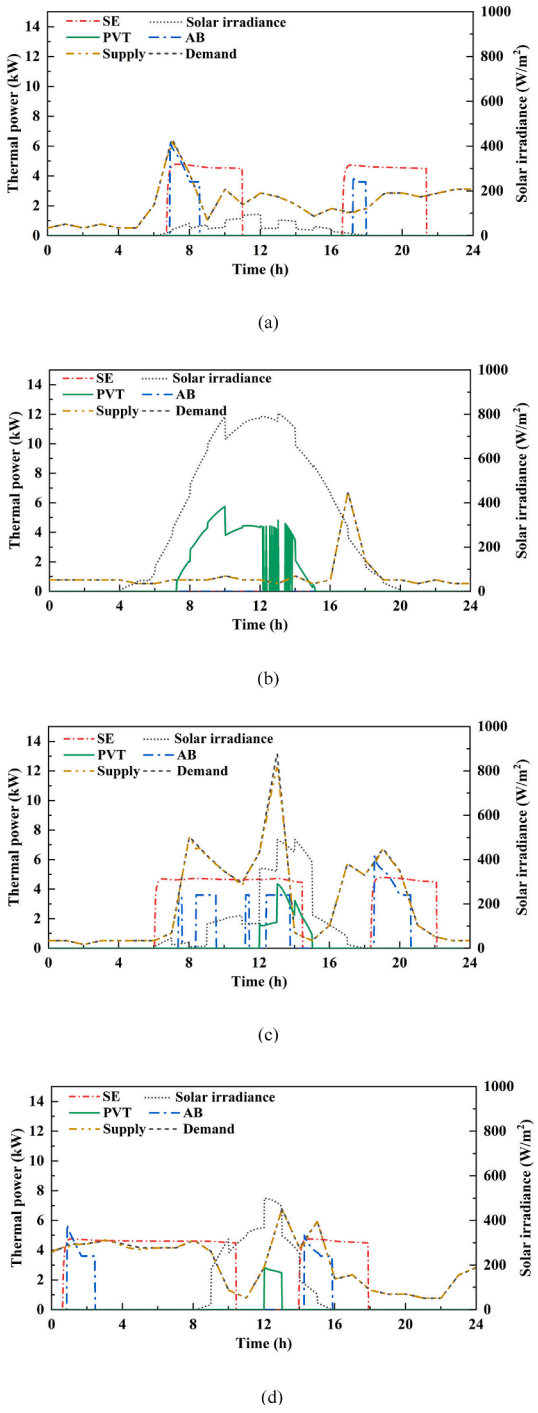

Fig. 13. Generated, supplied, and demand thermal power, and solar irradiance during the four typical days: (a) 21st March, (b) 21st June, (c) 21st September, and (d) 21st December.

electricity and the surplus power is exported to the grid. From 16:30 pm, the load demand is larger than the output electric power generated by the PVT, the electricity stored in the battery is discharged to match demands, and there is no need to import electricity from the grid, till the end of this day. However, in winter, the output electric power generated by the PVT is quite lower than that in summer. Though the SE will also contribute to service either power demand or charging the battery, importing electricity from the grid is still required in the evening after the battery is deactivated (the SoC of the battery reaches the low limit value). In comparison with the heat self-sufficiency of the proposed CHP system, the electricity self-sufficiency is lower since importing electricity from the grid is required on all four typical days. The main reason is that the SE micro-CHP unit is configured for heat-led control, which first prioritises to fulfil the heat demand rather than the electricity demand.(a).

4.2.2. Monthly operating characteristics and comparison with the reference system

Fig. 15(a) further accumulates the monthly generated, supplied and demand thermal energy. For the PVT collectors, the maximum heat generated is 680 kWh in April, and the minimum heat generated is 80 kWh in December. While for the SE, the maximum heat generated is 3110 kWh in December, and the minimum heat generated is 13 kWh in July. The maximum heat generated by the AB is 640 kWh in January and the AB is unused in August. According to Fig. 15(a), we can also see that the integration of the SE micro-CHP unit with the PVT collectors is able to fulfil the heat load demand completely in each month. The annual thermal energy demand coverage of the micro-CHP system is 99.5%. In addition, the yearly heat contribution of the PVT collector, SE and AB are 4510 kWh (19.8% of the total heat generated by the micro-CHP system), 14,500 kWh (63.6%), and 3760 kWh (16.5%), respectively.

Fig. 15(b) shows the monthly generated, supplied, and exported electricity. The maximum (total) electrical energy generated by the PVT collectors is 420 kWh in July while the minimum one is 100 kWh in December. For the SE, the maximum electrical energy generated is 620 kWh in December, and there is no net electricity production in both July and August. In contrast to the monthly heat production of the micro-CHP system, though the electricity production of the system is higher than the electrical load demand in each month, the monthly electricity production is unable to meet the electrical load demand completely (with annual electricity self-sufficiency of 87.2%) due to the mismatch between electricity production and electricity consumption (which has been discussed before). The maximum electricity deficit (the gap between the electricity demand curve and the onsite use electricity curve) occurs in September, in which 80 kWh of electricity is imported from the grid. As expected, the micro-CHP system can also export surplus electricity to the grid to accrue revenue, and the maximum electricity export of 160 kWh occurs in April.

Generally, fuel cost accounts for a large proportion of the operating costs of a CHP system. Fig. 15(c) presents the comparison of the monthly gas consumption of the micro-CHP system and the reference system. In winter months, the monthly gas consumption of the micro-CHP system is higher than that of the reference system, while in summer months, the monthly gas consumption of the micro-CHP system is lower than that of the reference system due to the contribution of solar energy. The annual gas consumption of the micro-CHP system and the reference system are 23,800 and 25,800 kWh, respectively. Fig. 15(d) further gives the monthly operating cost and carbon emissions of the two different systems. The highest monthly saving achieved by the micro-CHP system is in December at £90 and the lowest in September at £60. The annual operating saving is £900. As for the monthly carbon emission reduction achieved by the micro-CHP system, it depends strongly on the contribution of solar energy, as shown by the gap between the carbon emission curves of the two different systems. The higher the contribution of solar energy, the more the monthly carbon emission reduction is achieved by the micro-CHP system. The highest carbon emission reduction achieved by the micro-CHP system is in April with 300 $kgCO_{2\text{-eq}}$ and the lowest in January with 150 $kgCO_{2\text{-eq}}$. The annual carbon emission reduction is 2480 $kgCO_{2\text{-eq}}$, corresponding to an annual carbon emission reduction rate of 37%.

Finally, Table 7 summarises the economic and carbon emission comparison results of the micro-CHP system against the reference system. It can be seen that though both the carbon emission savings and annual operating saving potentials of the micro-CHP system are significant, the discounted payback period of 28 years is quite long, which approaches the total operation period of 30 years. The main reason behind this is the capital cost of such a micro-CHP system is

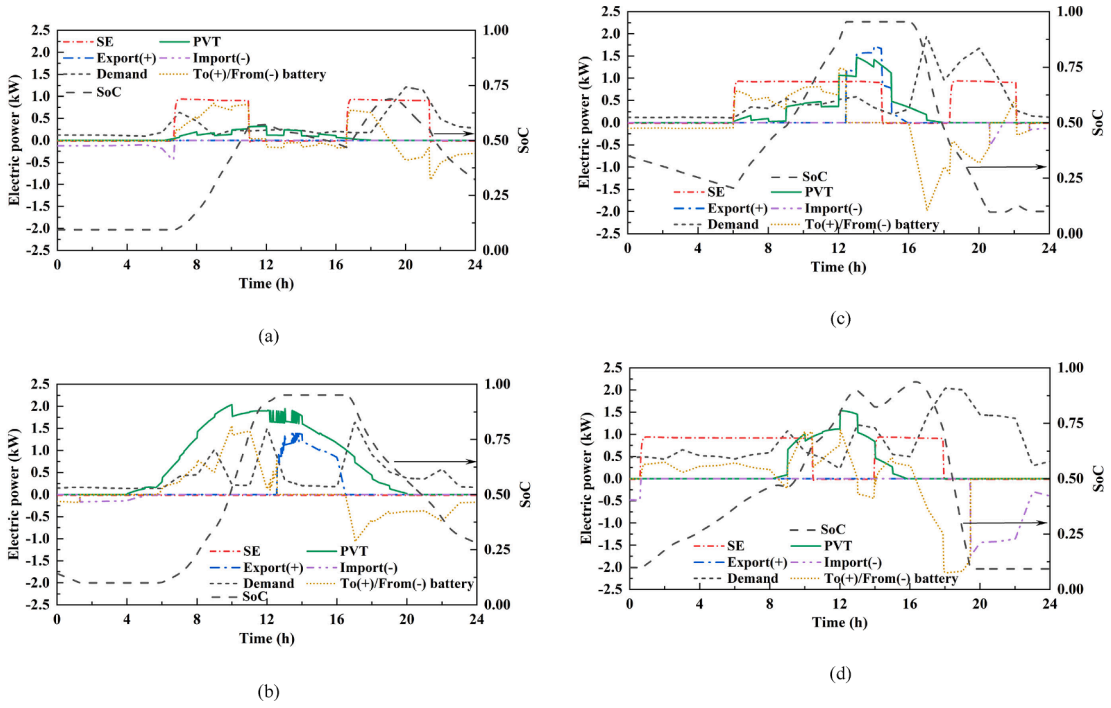

Fig. 14. Generated, supplied and demand electric power, and SoC of the battery during the four typical days: (a) 21st March, (b) 21st June, (c) 21st September and (d) 21st December.

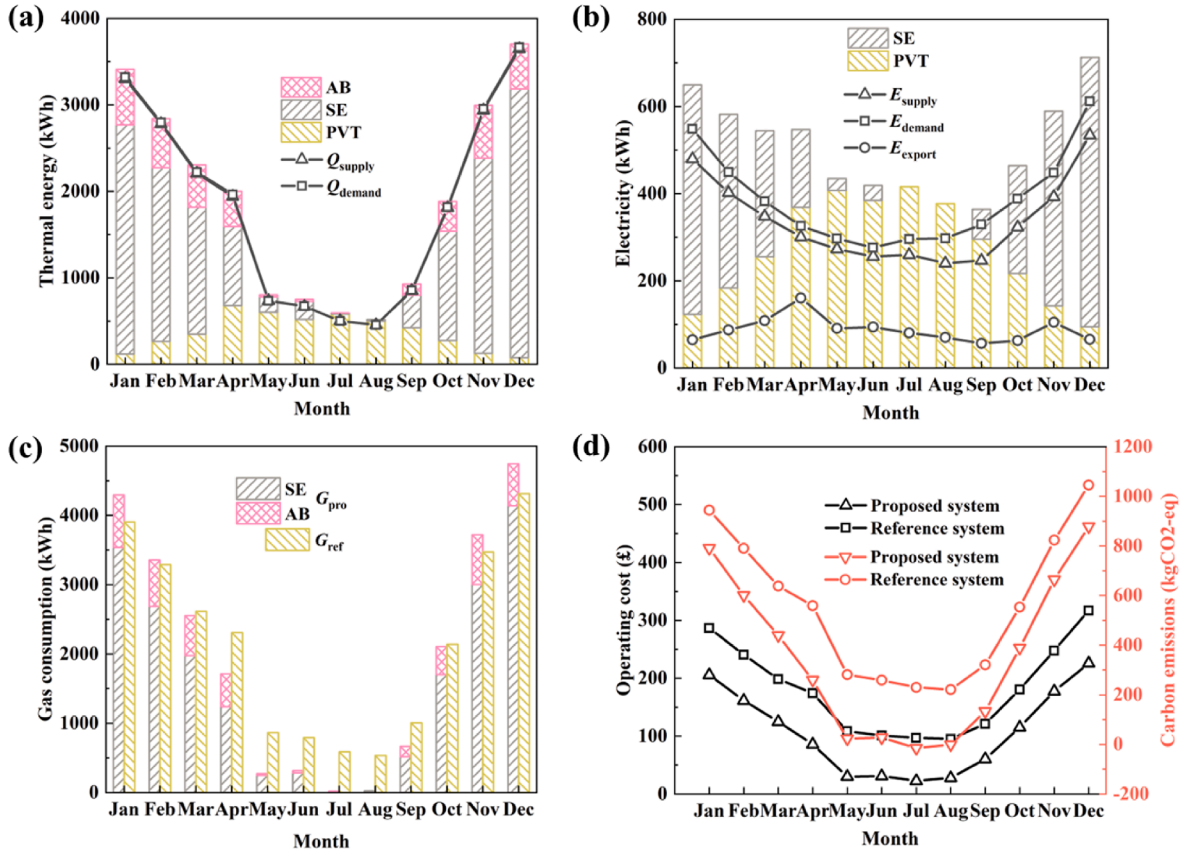

Fig. 15. (a) Monthly generated, supplied and demand thermal energy, (b) monthly generated, supplied and exported electricity, (c) monthly gas consumption of the micro-CHP system and the reference system, and (d) monthly operating cost and carbon emissions of the micro-CHP system and the reference system.

Table 7
Summary of the economic and emission comparison results.

	Reference system	Proposed system
Revenue		
Annual exported electricity (£)	0	50
Costs		
Annual maintenance cost (£)	120	220
Annual natural gas cost (£)	1060	980
Annual imported electricity cost (£)	990	130
Annual total operating cost (£)	2170	1270
Capital cost (£)	2500	17,200
Incremental capital cost (£)	0	14,700
Incremental replacement cost (£)	0	7730
Economic appraisal		
Discounted payback period (years)	0	28
Net present value (£)	0	1990
Carbon emission appraisal		
Annual carbon emission ($kgCO_{2\text{-}eq}$)	6670	4190
Annual carbon emission reduction ($kgCO_{2\text{-}eq}$)	0	2480
Annual carbon emission reduction rate	0	37%

considerable, which is 6.9 times that of a traditional system. The high capital cost mainly arises from the SE micro-CHP unit and the PVT collectors, which account for 43% and 27% of the total capital cost, respectively. So, it is anticipated that further reducing the capital cost of the SE micro-CHP unit and the PVT collectors will make this CHP technology more viable.

4.3. Comparison with alternative solar cogeneration systems

In this section, the energetic, economic and environmental potential of the proposed micro-CHP system is further compared to that of some alternative solar-based systems, to evaluate the pros and cons of the proposed system comprehensively. The alternative systems considered here include a PV-only system, a standalone PVT system, and a PVT-assisted heat pump system, all of which are connected to the electricity grid and supplemented by a conventional gas-fired boiler.

The PV-only system considered here was designed for electricity provision to a three-bedroom terraced house (with 15 m^2 of available roof area for PV installation) in London (UK), aiming to reduce imported electricity form the grid, and both electricity and heat storage were not included in the system [2,60]. The standalone PVT system was developed for heat (including both DHW and SH) and electricity provision to a semi-detached house (with a total floor area of ~115 m^2), also located in London, and both the electricity and heat storage were considered [42]. While the PVT-assisted heat pump system was investigated for DHW and electricity provision to a three-bedroom terraced house in Belfast, UK (with an almost identical northern climate as London) [55], and the considered PVT installation area was 28 m^2, which is close to that in this work. Electricity storage was not considered in the PVT-assisted heat pump system. Generally, different installed areas of solar systems and households energy demands will influence the performance of these systems [21], however, the comparison is still reasonable for the four different systems since all of them are being studied in the UK energy system, based on the same (domestic) application, with similar system sizes and end-user demands, and assessed under almost identical climates.

Table 8 shows the energetic, economic and carbon emission comparison results between the three alternative systems and the proposed micro-CHP system. It should be noted that among the four analysed systems here, only the proposed system in this work considers component replacement cost. In comparison with the PV-only system, the standalone PVT system enables a higher heat demand coverage due to the heat production of the PVT collector, which also enhances its annual carbon emission reduction potential. The annual gross electricity production by the standalone PVT system is slightly higher than that of the

Table 8
Energetic, economic and carbon emission comparison results between the three alternative systems and the proposed micro-CHP system.

	PV-only system [2,60]	PVT system [42]	PVT-assisted heat pump system [55]	Proposed micro-CHP system
Targeted house type	Terraced house	Semi-detached house	Terraced house	Detached house
Installed area (m^2)	15	17	27	28
Panel number	9	11	20	18
Annual household electricity demand (kWh)	4500	2790	3810	4650
Annual household heat demand (kWh)	2880 (DHW-only)*	6290	2550 (DHW-only)*	22,000
Gross electricity production (kWh)	2190	3030	4040	3260 (PVT) + 2820 (SE)
Electricity self-sufficiency	48.7%	65.6%	34.0%	87.2%
Heat production (kWh)	0	1630	2080	4510 (PVT) + 14500 (SE)
Heat demand coverage	0	29.3%	82.0% (DHW-only)	83.4%**
Heat produced by AB (kWh)	2880 + Q_{SH}	3940	460 + Q_{SH}	3760
Estimated capital cost (£)	4270	7240	15,940	17,200
Annual carbon emission reduction (kgCO2-eq)	590	1650	1370	2480
Payback time (years)	7	23	18	28

* With no information for SH.
**The contribution of AB is excluded herein.

PV-only system due to the cooling of the PV cells (which allows a slight increase in the operating efficiency of the PV cells) if the installed areas of the two systems are identical (a larger installed area of the standalone PVT system than that of the PV-only system herein is another reason for the increase of the annual gross electricity production by the standalone PVT system) [65]. When compared to the standalone PVT system, the proposed system in this work allows much higher electricity self-sufficiency and heat demand coverage, thanks to the contribution of the SE micro-CHP unit. Since the use of a SE micro-CHP unit allows primary energy saving and carbon emission reduction in comparison with a conventional system including gas boiler and grid electricity [20], the carbon emission reduction and primary energy saving potentials for a standalone PVT system will be further increased if the auxiliary gas boiler in the standalone PVT system is replaced into a SE micro-CHP unit. However, such a retrofit will lead to a significant increase in the capital cost (£7240 vs. £17200) and the payback time (23 years vs. 28 years) due to the considerable capital cost of the SE micro-CHP unit, as shown in Table 8.

The comparison between the PVT-assisted heat pump system and the proposed CHP system is more complex: the former boosts the thermal output of a standalone PVT system, but with the expense of the consumption of an amount of electricity for the compressor of the heat pump; while the latter enhances both the thermal and electrical output of a standalone PVT system, but with the expense of the consumption of an amount of natural gas. As can be seen in Table 8, for a household with higher annual heat demand, the proposed system outperforms better than that of the PVT-assisted heat pump system in terms of potential environmental benefits (annual carbon emission reduction 1370 $kgCO_{2\text{-}eq}$ vs. 2480 $kgCO_{2\text{-}eq}$). The possible reason behind this is that the the carbon emission of electricity are significantly higher than that of natural gas (however, with a further decarbonization of grid electricity, the

comparison results may be changed). While due to the higher capital cost of the SE unit than that of a heat pump (£7370 vs. £2730) [55], meanwhile both electricity storage and component replacement cost were not considered in the assessment of the PVT-assisted heat pump system in Ref. [55], the payback time of the proposed system is longer than that of the PVT-assisted heat pump system (28 years vs. 18 years).

Therefore, in a UK context, choosing a suitable alternative system from the four analysed options will depend on the specific end-user needs. If the end-users pursue a shorter payback time, the PV-only system is preferred, whereas if the focus is on the potential environmental benefits of the alternative system rather than the initial cost, the proposed micro-CHP system would be a good option especially when the household has a higher annual heat demand.

4.4. Effect of utility prices

Results up to this point are based on fixed utility prices. However, the technical and economic feasibility of a CHP system depends greatly on utility prices. Hence the influence of utility prices on the micro-CHP system's economics is evaluated in this section. Since the electricity purchase price in the UK fluctuates between £0.127/kWh and £0.278/kWh from 2010 to 2022 [72], hence electricity purchase prices ranging from £0.1/kWh to £0.5/kWh are considered. The SEG tariff is assumed as 23% of the electricity purchase price, to keep consistent with the above analysis. In addition, natural gas prices ranging from £0.01/kWh to £0.15/kWh is studied based on the natural gas price variation from 2010 to 2022 [60,73–75].

Fig. 16(a) shows the effect of the electricity purchase price on the NPV and payback period of the micro-CHP system at a fixed natural gas price. It is observed that the electricity purchase price has a significant effect on the micro-CHP system's economics. With the increase in the electricity purchase price, the NPV increases linearly and the payback period declines accordingly. When the electricity purchase price is lower than £0.2/kWh (for example the electricity purchase price in 2010), the NPV is negative and the investment will never be paid back. When the electricity purchase price rises from £0.213/kWh to £0.4/kWh (increased by 88%), the NPV increases from £1990 to £22800 (increased by 10.5 times), and the payback period is shortened from 28 to 10 years. Thanks to the high ESS the micro-CHP system could achieve, with the increase of the electricity purchase price, the annual operating cost saving goes up sharply, hence a better economic performance can be achieved.

Fig. 16(b) presents the effect of natural gas price on the NPV and payback period of the micro-CHP system at a fixed electricity purchase price. It can be seen that the investment for the micro-CHP system gets recovered during the total operation period of 30 years, for all of the studied natural gas prices. With the increase in natural gas price, the NPV increases gradually and the payback period declines accordingly. When the natural gas price rises from £0.041/kWh to £0.15/kWh (increased by 2.7 times), the NPV increases from £1990 to £ 7760 (increased by 2.9 times), and the payback period is shortened from 28 to 22 years. In contrast to the electricity purchase price, the natural gas price has a moderate effect on the micro-CHP system's economics. The reason behind this is the annual gas consumption saving achieved by the micro-CHP system is only 2000 kWh (see Fig. 14 (c)), which is far less than the annual saving for electricity purchase from the grid (4060 kWh); given the natural gas price is cheaper than the electricity purchase price, hence the electricity purchase price plays a more important role in determining the economic performance of the micro-CHP system.

Table 9 shows the economic results of the proposed micro-CHP system for different utility-price scenarios in the UK. It can be seen that the economics of the system is very sensitive to utility prices. If utility prices are identical to that of 2010, the system will not generate profits during the total operation period of 30 years. When the utility prices are identical to that of early 2023, the system is expected to generate profits after 11 years of operation. This implies the proposed micro-CHP system emerges as a promising decarbonisation solution if utility prices increase, which is occurring given recent trends.

5. Conclusions

A small-scale (domestic) system integrating 29.5 m^2 of hybrid photovoltaic-thermal collectors, a 1-kW_e Stirling engine and energy storage for combined heat and power provision was studied comprehensively from energetic, economic and environmental perspectives. A parametric sensitive analysis aimed at assessing the effect of collector flow rate, storage tank size, SE micro-CHP flow rate, and battery capacity was performed. This was complemented by an evaluation of the daily and monthly operating characteristics of the proposed system for

Table 9
Economic results for different utility-price scenarios in the UK.

Utility-price scenarios	Prices in 2010	Prices in 2021	Prices in 2022	Prices in early 2023
Electricity purchase price, £/kWh	0.127 [72]	0.213 [59]	0.278 [72]	0.340 [72]
Natural gas price, £/kWh	0.036 [73]	0.041 [60]	0.083 [74]	0.103 [75]
NPV, £	−7900	1990	11,400	19,400
Payback period, years	–	28	18	11

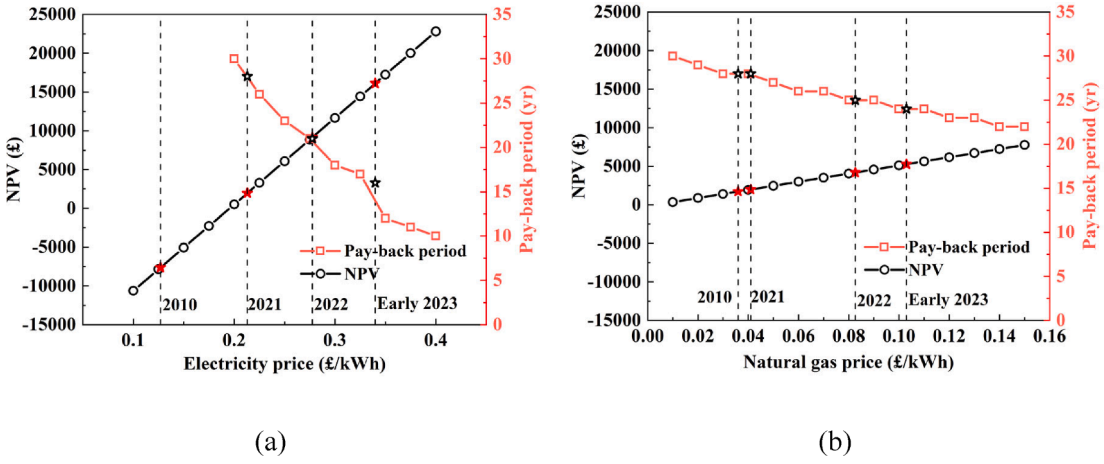

Fig. 16. (a) NPV and payback period with different electricity purchase prices at a fixed natural gas price of £0.041/kWh, and (b) NPV and payback period with different natural gas prices at a fixed electricity purchase price of £0.213/kWh.

selected component sizes and operating parameters. The performance of the system was then compared to that of a reference system (gas boiler plus grid electricity).

It is concluded that the collector flow rate does not strongly influence the thermal output of the system, but it does affect its electrical generation potential. When the collector flow rate is zero or close to zero, both the economic viability and the carbon emission savings potential of such a system are low. In addition, the storage tank size does not notably influence the electricity and heat generation of the proposed system since the SE micro-CHP unit and the PVT collectors are used in a synergistic manner. However, the storage tank size still needs to be selected carefully to achieve a high NPV, since the capital cost of the storage tank is considerable when the tank size is large. A lower water flow rate through the SE unit is beneficial for better economic viability and carbon emission savings since more electricity is generated from the SE and the PVT collectors at lower water flow rates; however, the annual thermal energy demand coverage is reduced at lower flow rates. The battery capacity only influences the electricity generation profile of the system, and there is an optimal capacity that maximises the economic viability of the system.

Further analysis indicates that the use of an optimised micro-CHP system in a detached house located in London (UK) can achieve an annual electricity self-sufficiency of 87.2% and an annual thermal energy demand coverage of 99.5%, respectively. The lower annual electricity self-sufficiency arises from the mismatch between electricity production and demand. The annual primary energy saving, carbon emission reduction rate, and operating cost saving are 35%, 37% and £900 relative to the reference system. Over 30 years of operation, the NPV of the proposed system is £1990 and the discounted payback period is 28 years. Relative to alternative solar-based systems, including a PVT-assisted heat pump system and a standalone PVT system, the proposed solar micro-CHP system offers greater potential environmental benefits but has a longer payback period. Furthermore, the economic viability of the system is very sensitive to utility prices, especially the electricity purchase price. Based on the utility prices in early 2023, the payback time of the system reduces to 11 years.

Together the above results imply that although the primary energy saving and the carbon emission reduction potential of the proposed micro-CHP system are significant, the initial investment/capital costs of such a system are high, especially arising from the SE micro-CHP unit and the PVT collector array, which acts as a barrier to widespread penetration at present. If a further reduction of the initial investment, especially the PVT collectors and the SE micro-CHP unit costs, can be achieved, this will significantly reduce the payback time and attract the widespread deployment of this technology. An increase in utility prices will further shorten the payback time of this and other similar systems. Finally, if the SE micro-CHP unit can be fuelled by biomass, this would make the proposed system a fully renewable heat and electricity supply system, with additional financial and environmental benefits.

CRediT authorship contribution statement

Shunmin Zhu: Conceptualization, Funding acquisition, Methodology, Investigation, Formal analysis, Software, Writing - original draft. **Kai Wang:** Investigation, Software. **Iker González-Pino:** Investigation, Software. **Jian Song:** Writing – review & editing. **Guoyao Yu:** Funding acquisition. **Ercang Luo:** Funding acquisition, Supervision, Resources. **Christos N. Markides:** Funding acquisition, Supervision, Resources, Writing – review & editing.

Declaration of Competing Interest

The authors declare that they have no known competing financial interests or personal relationships that could have appeared to influence the work reported in this paper.

Data availability

Data will be made available on request.

Acknowledgments

This work was supported by the International Postdoctoral Exchange Fellowship Program of the Office of China Postdoc Council (Grant No. 2020051). This work was also supported by the UK Engineering and Physical Sciences Research Council (EPSRC) [grant numbers EP/M025012/1, and EP/R045518/1], and by the Royal Society via an International Collaboration Award 2020 [grant number ICA\R1\201302]. The authors would like to thank UK company Solar Flow Ltd. (www.solar-flow.co.uk). Data supporting this publication can be obtained on request from cep-lab@imperial.ac.uk. For the purpose of Open Access, the authors have applied a CC BY public copyright licence to any Author Accepted Manuscript version arising from this submission.

References

[1] Bell M, Gault A, Thompson M, Hill J, Joffe D. Next steps for UK heat policy, Committee on Climate Change: London, UK, 2016. URL: https://www.theccc.org.uk/publication/next-steps-for-uk-heat-policy/.
[2] Herrando M, Markides CN. Hybrid PV and solar-thermal systems for domestic heat and power provision in the UK: Techno-economic considerations. Appl Energy 2016;161:512–32. https://doi.org/10.1016/j.apenergy.2015.09.025.
[3] Guarracino I, Mellor A, Ekins-Daukes NJ, Markides CN. Dynamic coupled thermal-and-electrical modelling of sheet-and-tube hybrid photovoltaic/thermal (PVT) collectors. Appl Therm Eng 2016;101:778–95. https://doi.org/10.1016/j.applthermaleng.2016.02.056.
[4] Chow TT, Pei G, Fong K, Lin Z, Chan A, Ji J. Energy and exergy analysis of photovoltaic–thermal collector with and without glass cover. Appl Energy 2009;86:310–6. https://doi.org/10.1016/j.apenergy.2008.04.016.
[5] Guarracino I, Freeman J, Ramos A, Kalogirou SA, Ekins-Daukes NJ, Markides CN. Systematic testing of hybrid PV-thermal (PVT) solar collectors in steady-state and dynamic outdoor conditions. Appl Energy 2019;240:1014–30. https://doi.org/10.1016/j.apenergy.2018.12.049.
[6] Herrando M, Ramos A, Zabalza I, Markides CN. A comprehensive assessment of alternative absorber-exchanger designs for hybrid PVT-water collectors. Appl Energy 2019;235:1583–602. https://doi.org/10.1016/j.apenergy.2018.11.024.
[7] Huang G, Wang K, Curt SR, Franchetti B, Pesmazoglou I, Markides CN. On the performance of concentrating fluid-based spectral-splitting hybrid PV-thermal (PV-T) solar collectors. Renew Energy 2021;174:590–605. https://doi.org/10.1016/j.renene.2021.04.070.
[8] Huang G, Curt SR, Wang K, Markides CN. Challenges and opportunities for nanomaterials in spectral splitting for high-performance hybrid solar photovoltaic-thermal applications: a review. Nano Mater Sci 2020;2:183–203. https://doi.org/10.1016/j.nanoms.2020.03.008.
[9] Herrando M, Pantaleo AM, Wang K, Markides CN. Solar combined cooling, heating and power systems based on hybrid PVT, PV or solar-thermal collectors for building applications. Renew Energy 2019;143:637–47. https://doi.org/10.1016/j.renene.2019.05.004.
[10] Wang K, Herrando M, Pantaleo AM, Markides CN. Technoeconomic assessments of hybrid photovoltaic-thermal vs. conventional solar-energy systems: Case studies in heat and power provision to sports centres. Appl Energy 2019;254:113657. 10.1016/j.apenergy.2019.113657.
[11] Wang K, Pantaleo AM, Herrando M, Faccia M, Pesmazoglou I, Franchetti BM, et al. Spectral-splitting hybrid PV-thermal (PVT) systems for combined heat and power provision to dairy farms. Renew Energy 2020;159:1047–65. https://doi.org/10.1016/j.renene.2020.05.120.
[12] Ramos A, Chatzopoulou MA, Guarracino I, Freeman J, Markides CN. Hybrid photovoltaic-thermal solar systems for combined heating, cooling and power provision in the urban environment. Energy Convers Manage 2017;150:838–50. https://doi.org/10.1016/j.enconman.2017.03.024.
[13] National Grid, Solar PV Briefing Note, DECC, Editor. DECC: London, 2012.
[14] Edmunds R, Cockerill T, Foxon T, Ingham D, Pourkashanian M. Technical benefits of energy storage and electricity interconnections in future British power systems. Energy 2014;70:577–87. https://doi.org/10.1016/j.energy.2014.04.041.
[15] Martinez S, Michaux G, Salagnac P, Bouvier J-L. Micro-combined heat and power systems (micro-CHP) based on renewable energy sources. Energy Convers Manage 2017;154:262–85. https://doi.org/10.1016/j.enconman.2017.10.035.
[16] Pehnt M, Cames M, Fischer C, Praetorius B, Schneider L, Schumacher K, et al. Micro cogeneration towards dencentralized energy systems. Springer, Berlin;2006. p. 1-16.
[17] Zhu S, Yu G, Jongmin O, Xu T, Wu Z, Dai W, et al. Modeling and experimental investigation of a free-piston Stirling engine-based micro-combined heat and power system. Appl Energy 2018;226:522–33. https://doi.org/10.1016/j.apenergy.2018.05.122.

[18] Jiang Z, Yu G, Zhu S, Dai W, Luo E. Advances on a free-piston Stirling engine-based micro-combined heat and power system. Appl Therm Eng 2022;217:119187. https://doi.org/10.1016/j.applthermaleng.2022.119187.

[19] Zhu S, Yu G, Ma Y, Cheng Y, Wang Y, Yu S, et al. A free-piston Stirling generator integrated with a parabolic trough collector for thermal-to-electric conversion of solar energy. Appl Energy 2019;242:1248–58. https://doi.org/10.1016/j.apenergy.2019.03.169.

[20] Zhu S, Yu G, Liang K, Dai W, Luo E. A review of Stirling-engine-based combined heat and power technology. Appl Energy 2021;294:116965. https://doi.org/10.1016/j.apenergy.2021.116965.

[21] Balcombe P, Rigby D, Azapagic A. Energy self-sufficiency, grid demand variability and consumer costs: Integrating solar PV, Stirling engine CHP and battery storage. Appl Energy 2015;155:393–408. https://doi.org/10.1016/j.apenergy.2015.06.017.

[22] Brandoni C, Renzi M. Optimal sizing of hybrid solar micro-CHP systems for the household sector. Appl Therm Eng 2015;75:896–907. https://doi.org/10.1016/j.applthermaleng.2014.10.023.

[23] Rodríguez LR, Lissén JMS, Ramos JS, Jara EÁR, Domínguez SÁ. Analysis of the economic feasibility and reduction of a building's energy consumption and emissions when integrating hybrid solar thermal/PV/micro-CHP systems. Appl Energy 2016;165:828–38. https://doi.org/10.1016/j.apenergy.2015.12.080.

[24] Shah KK, Mundada AS, Pearce JM. Performance of US hybrid distributed energy systems: Solar photovoltaic, battery and combined heat and power. Energy Convers Manage 2015;105:71–80. https://doi.org/10.1016/j.enconman.2015.07.048.

[25] Mundada AS, Shah KK, Pearce JM. Levelized cost of electricity for solar photovoltaic, battery and cogen hybrid systems. Renew Sustain Energy Rev 2016;57:692–703. https://doi.org/10.1016/j.rser.2015.12.084.

[26] Karmacharya S, Putrus G, Underwood C, Mahkamov K, McDonald S, Alexakis A. Simulation of energy use in buildings with multiple micro generators. Appl Therm Eng 2014;62(2):581–92. https://doi.org/10.1016/j.applthermaleng.2013.09.039.

[27] Jimenez Zabalaga P, Cardozo E, Choque Campero LA, Araoz Ramos JA. Performance analysis of a stirling engine hybrid power system. Energies 2020;13(4):980. https://doi.org/10.3390/en13040980.

[28] Kotowicz J, Uchman W. Analysis of the integrated energy system in residential scale: Photovoltaics, micro-cogeneration and electrical energy storage. Energy 2021;227:120469. https://doi.org/10.1016/j.energy.2021.120469.

[29] Balcombe P, Rigby D, Azapagic A. Environmental impacts of microgeneration: Integrating solar PV, Stirling engine CHP and battery storage. Appl Energy 2015;139:245–59. https://doi.org/10.1016/j.apenergy.2014.11.034.

[30] Auñón-Hidalgo JA, Sidrach-de-Cardona M, Auñón-Rodríguez F. Performance and CO2 emissions assessment of a novel combined solar photovoltaic and thermal, with a Stirling engine micro-CHP system for domestic environments. Energy Convers Manage 2021;230:113793. https://doi.org/10.1016/j.enconman.2020.113793.

[31] İncili V, Dolgun GK, Georgiev A, Keçebaş A, Çetin NS. Performance evaluation of novel photovoltaic and Stirling assisted hybrid micro combined heat and power system. Renew Energy 2022;189:129–38. https://doi.org/10.1016/j.renene.2022.03.030.

[32] Kallio S, Siroux M. Exergy and exergo-economic analysis of a hybrid renewable energy system under different climate conditions. Renew Energy 2022;194:396–414. https://doi.org/10.1016/j.renene.2022.05.115.

[33] Stamford L, Greening B, Azapagic A. Life cycle environmental and economic sustainability of Stirling engine micro-CHP systems. Energy Technol 2018;6(6):1119–38. https://doi.org/10.1002/ente.201700854.

[34] https://www.ofgem.gov.uk/environmental-and-social-schemes/smart-export-guarantee-seg.

[35] González-Pino I, Pérez-Iribarren E, Campos-Celador A, Terés-Zubiaga J, Las-Heras-Casas J. Modelling and experimental characterization of a Stirling engine-based domestic micro-CHP device. Energy Convers Manage 2020;225:113429. https://doi.org/10.1016/j.enconman.2020.113429.

[36] Baxi, Ecogen: The Baxi Ecogen Dual Energy System, 2011.

[37] Chen Y, Yang Z, Wang Y. SOC estimation of lead carbon batteries based on the operating conditions of an energy storage system in a microgrid system. Energies 2019;13(1):33. https://doi.org/10.3390/en13010033.

[38] Energy Saving Trust E. Solar Energy Calculator Sizing Guide. 2011.

[39] Photovoltaic geographical information system (PVGIS). https://joint-research-centre.ec.europa.eu/pvgis-online-tool_en.

[40] González-Pino I. Modelling, experimental characterization and simulation of Stirling engine-based micro-cogeneration plants for residential buildings Universidad del País Vasco -. Euskal Herriko Unibertsitatea 2019.

[41] S.A. Klein et al, TRNSYS 17: A Transient System Simulation program, Solar Energy Laboratory, University of Wisconsin, Madison, USA, Trnsys. (2010). http://sel.me.wisc.edu/trnsys.

[42] Herrando M, Ramos A, Freeman J, Zabalza I, Markides CN. Technoeconomic modelling and optimisation of solar combined heat and power systems based on flat-box PVT collectors for domestic applications. Energy Convers Manage 2018;175:67–85. https://doi.org/10.1016/j.enconman.2018.07.045.

[43] Yu Y, Long E, Chen X, Yang H. Testing and modelling an unglazed photovoltaic thermal collector for application in Sichuan Basin. Appl Energy 2019;242:931–41. https://doi.org/10.1016/j.apenergy.2019.03.114.

[44] anister CJ, Wagar WR, Collins MR. Validation of a single tank, multi-mode solar-assisted heat pump TRNSYS model. Energy Procedia 2014;48:499-504. 10.1016/j.egypro.2014.02.059.

[45] Baldwin C, Cruickshank CA. Using TRNSYS types 4, 60, and 534 to model residential cold thermal storage using water and water/glycol solutions. Proceedings of the IBPSA-Canada's eSim Conference, Hamilton, ON, Canada2016. p. 1-11. http://www.ibpsa.org/proceedings/eSimPapers/2016/52-77-eSim2016.pdf.

[46] UK Energy Research Centre Energy Data Centre (UKERC-EDC), Milton Keynes Energy Park Dwellings. URL: https://data.ukedc.rl.ac.uk/browse/edc/efficiency/residential/Buildings/MiltonKeynesEnergyPark_1990.

[47] Jing R, Zhou Y, Wu J. Electrification with flexibility towards local energy decarbonization. Adv Appl Energy 2022;5:100088. https://doi.org/10.1016/j.adapen.2022.100088.

[48] Gillich A, Godefroy J, Ford A, Hewitt M, L'Hostis J. Performance analysis for the UK's first 5th generation heat network–The BEN case study at LSBU. Energy 2022;243:122843. https://doi.org/10.1016/j.energy.2021.122843.

[49] https://www.statista.com/statistics/548943/thermal-efficiency-gas-turbine-stations-uk/.

[50] Lamnatou C, Chemisana D. Photovoltaic/thermal (PVT) systems: A review with emphasis on environmental issues. Renew Energy 2017;105:270–87. https://doi.org/10.1016/j.renene.2016.12.009.

[51] Dubey S, Tiwari GN. Analysis of PV/T flat plate water collectors connected in series. Sol Energy 2009;83(9):1485–98. https://doi.org/10.1016/j.solener.2009.04.002.

[52] González-Pino I, Campos-Celador A, Pérez-Iribarren E, Terés-Zubiaga J, Sala J. Parametric study of the operational and economic feasibility of Stirling micro-cogeneration devices in Spain. Appl Therm Eng 2014;71(2):821–9. https://doi.org/10.1016/j.applthermaleng.2013.12.020.

[53] Sangwongwanich A, Yang Y, Sera D, Blaabjerg F. Lifetime evaluation of grid-connected PV inverters considering panel degradation rates and installation sites. IEEE Trans Power Electron 2017;33(2):1225–36. https://doi.org/10.1109/TPEL.2017.2678169.

[54] Solar Guide, Compare Smart Export Guarentee Tariffs, 2022. URL: https://www.solarguide.co.uk/smart-export-guarantee-comparison#/.

[55] Obalanlege MA, Xu J, Markides CN, Mahmoudi Y. Techno-economic analysis of a hybrid photovoltaic-thermal solar-assisted heat pump system for domestic hot water and power generation. Renew Energy 2022;196:720–36. https://doi.org/10.1016/j.renene.2022.07.044.

[56] Stovesandsolar. https://www.stovesandsolar.com/.

[57] Solax 5.0kW Boost Inverter (model: SL-X1BOOST-5.0T). https://www.stovesandsolar.com/product-page/solax-5-0kw-inverter.

[58] Victron Energy Lead Carbon Battery, https://www.selectsolar.co.uk/cat/227/select-solar-lead-acid-battery-range.

[59] Statista. Electricity prices for households in the United Kingdom. 2021. https://www.statista.com/statistics/418126/electricity-prices-for-households-in-the-uk.

[60] DECC. Annual domestic energy bills (QEP 2.3.4). 2021. https://www.gov.uk/government/statistical-data-sets/annual-domestic-energy-price-statistics.

[61] HM Treasury – Public Service Transformation Network. Supporting public service transformation: Cost benefit analysis guidance for local partnerships; 2014.

[62] Kalogirou SA, Tripanagnostopoulos Y. Hybrid PV/T solar systems for domestic hot water and electricity production. Energy Convers Manage 2006;47(18–19):3368–82. https://doi.org/10.1016/j.enconman.2006.01.012.

[63] Cui Z, Latif E, Stevenson V. Decision-making framework to identify the optimal hybrid renewable energy system for switching UK representative domestic buildings towards the net-zero target. 2022.

[64] Cossutta M, Foo DC, Tan RR. Carbon emission pinch analysis (CEPA) for planning the decarbonization of the UK power sector. Sustain Prod Consump 2021;25:259–70. https://doi.org/10.1016/j.spc.2020.08.013.

[65] Herrando M, Markides CN, Hellgardt K. A UK-based assessment of hybrid PV and solar-thermal systems for domestic heating and power: system performance. Appl Energy 2014;122:288–309. https://doi.org/10.1016/j.apenergy.2014.01.061.

[66] Bianchi M, De Pascale A, Spina PR. Guidelines for residential micro-CHP systems design. Appl Energy 2012;97:673–85. https://doi.org/10.1016/j.apenergy.2011.11.023.

[67] González-Pino I, Pérez-Iribarren E, Campos-Celador A, Terés-Zubiaga J. Analysis of the integration of micro-cogeneration units in space heating and domestic hot water plants. Energy 2020;200:117584. https://doi.org/10.1016/j.energy.2020.117584.

[68] Thiers S, Aoun B, Peuportier B. Experimental characterization, modeling and simulation of a wood pellet micro-combined heat and power unit used as a heat source for a residential building. Energy Build 2010;42(6):896–903. https://doi.org/10.1016/j.enbuild.2009.12.011.

[69] Bouvenot J-B, Andlauer B, Stabat P, Marchio D, Flament B, Latour B, et al. Gas Stirling engine μCHP boiler experimental data driven model for building energy simulation. Energy Build 2014;84:117–31. https://doi.org/10.1016/j.enbuild.2014.08.023.

[70] Purvins A, Papaioannou IT, Debarberis L. Application of battery-based storage systems in household-demand smoothening in electricity-distribution grids. Energy Convers Manage 2013;65:272–84. https://doi.org/10.1016/j.enconman.2012.07.018.

[71] McKenna E, McManus M, Cooper S, Thomson M. Economic and environmental impact of lead-acid batteries in grid-connected domestic PV systems. Appl Energy 2013;104:239–49. https://doi.org/10.1016/j.apenergy.2012.11.016.

[72] Average Cost of Electricity per kWh in the UK 2023. URL: https://www.nimblefins.co.uk/average-cost-electricity-kwh-uk.

[73] Statista. Household natural gas prices in the United Kingdom from 1995 to 2019. https://www.statista.com/statistics/1049319/household-natural-gas-price-united-kingdom/.
[74] DECC. Annual domestic energy bills (QEP 2.3.4). 2022. https://www.gov.uk/government/statistical-data-sets/annual-domestic-energy-price-statistics.
[75] https://www.gov.uk/government/publications/energy-bills-support/energy-bills-support-factsheet-8-september-2022.